



HAL
open science

OPTIMIZED SCHWARZ WAVEFORM RELAXATION METHOD FOR INCOMPRESSIBLE STOKES PROBLEM *

Duc-Quang Bui, Caroline Japhet, Pascal Omnes

► **To cite this version:**

Duc-Quang Bui, Caroline Japhet, Pascal Omnes. OPTIMIZED SCHWARZ WAVEFORM RELAXATION METHOD FOR INCOMPRESSIBLE STOKES PROBLEM *. 2023. hal-04105538

HAL Id: hal-04105538

<https://sorbonne-paris-nord.hal.science/hal-04105538>

Preprint submitted on 24 May 2023

HAL is a multi-disciplinary open access archive for the deposit and dissemination of scientific research documents, whether they are published or not. The documents may come from teaching and research institutions in France or abroad, or from public or private research centers.

L'archive ouverte pluridisciplinaire **HAL**, est destinée au dépôt et à la diffusion de documents scientifiques de niveau recherche, publiés ou non, émanant des établissements d'enseignement et de recherche français ou étrangers, des laboratoires publics ou privés.

1 **OPTIMIZED SCHWARZ WAVEFORM RELAXATION METHOD FOR**
2 **INCOMPRESSIBLE STOKES PROBLEM ***

3 DUC-QUANG BUI[‡] CAROLINE JAPHET[‡] AND PASCAL OMNES^{§‡}

4 **Abstract.** We propose and analyse the optimized Schwarz waveform relaxation (OSWR) method
5 for the unsteady incompressible Stokes equations. Well-posedness of the local subdomain problems
6 with Robin boundary conditions is proved. Convergence of the velocity is shown through energy
7 estimates; however, pressure converges only up to constant values in the subdomains, and an astute
8 correction technique is proposed to recover these constants from the velocity. The convergence factor
9 of the OSWR algorithm is obtained through a Fourier analysis, and allows to efficiently optimize
10 the space-time Robin transmission conditions involved in the OSWR method. Then, numerical
11 illustrations for the two-dimensional unsteady incompressible Stokes system are presented to illustrate
12 the performance of the OSWR algorithm.

13 **Key words.** Unsteady incompressible Stokes system, space-time domain decomposition, optimized
14 Schwarz waveform relaxation, Robin transmission conditions, correction technique for the pressure.

15 **AMS subject classifications.** 65M55, 35K45, 76D07, 65M12, 65M22, 65B99.

16 **1. Introduction.** The study of physical phenomena, whether natural or industrial,
17 is frequently based on numerical simulations involving an increasing number of degrees
18 of freedom. This growing complexity may require the use of resolution techniques
19 which on the one hand are suitable for parallel computing architectures, and on the
20 other hand allow local space and time stepping adapted to the physics, such as space-
21 time domain decomposition (DD) methods. In this article we are concerned with such
22 methods, with Robin transmission conditions at the interfaces between subdomains,
23 for solving applications related to incompressible fluid mechanics, that are modelled
24 by the unsteady (Navier)-Stokes system.

25 The well-posedness of such systems with Robin conditions (without domain de-
26 composition) has been the subject of several works in the steady case, see e.g. [47] for
27 the Stokes problem (where the Robin condition is expressed with the symmetric part
28 of the velocity gradient, instead of the gradient), references [45, 38] for the Oseen and
29 Navier-Stokes systems, and [16] for the Stokes-Darcy Coupling. On the other hand,
30 there are few works in the unsteady case; in [39] existence and uniqueness of a solution
31 with a time-dependent Robin boundary condition of the type $\text{curl } \mathbf{u} \times \mathbf{n} = \beta(t)\mathbf{u}$
32 is addressed. In [29] the Stokes problem with Robin conditions is studied, in the context
33 of a global-in-time DD method applied the coupled nonlinear Stokes and Darcy Flows.
34 The well-posedness is not shown.

35 In this article we study the well-posedness of the unsteady incompressible Stokes
36 system with Robin boundary conditions of type $\alpha(\nu\partial_{\mathbf{n}}\mathbf{u} \cdot \mathbf{n} - p) + \mathbf{u} \cdot \mathbf{n} = g(t)$ and
37 $\beta\nu\partial_{\mathbf{n}}\mathbf{u} \times \mathbf{n} + \mathbf{u} \times \mathbf{n} = \xi(t)$, in the context of space-time DD methods.

38 Concerning the DD approaches with Robin conditions, several studies have been
39 carried out for the incompressible (Navier)-Stokes equations : in [41, 42, 34, 43, 40] the
40 steady Oseen equation (and its application to the non-stationary Navier-Stokes equa-

***Funding:** The work of the authors was supported by the ANR project CINE-PARA under grant ANR-15-CE23-0019.

[‡]CNRS, UMR 7539, Laboratoire de Géométrie, Analyse et Applications, LAGA, Université Sorbonne Paris Nord, F-93430, Villetaneuse, France, (bui@math.univ-paris13.fr, japhet@math.univ-paris13.fr).

[§]Université Paris-Saclay, CEA, Service de Génie Logiciel pour la Simulation, 91191, Gif-sur-Yvette, France. (pascal.omnes@cea.fr).

41 tions, using a spatial DD at each time step) is considered. More precisely, in [42, 34, 43]
 42 a stabilized finite element approximation is proposed (with non-standard Robin con-
 43 ditions due to the stabilization). The convergence of the DD method is proven for the
 44 velocity. For the pressure, the convergence is proven when the original monodomain
 45 problem involves Robin boundary conditions on a part of the physical boundary.
 46 However, the authors point out that for an Oseen problem with Dirichlet conditions
 47 on the whole physical boundary, the pressure of the Robin-Robin DD algorithm will
 48 converge up to a constant which can differ for different subdomains. This important
 49 observation is also mentioned in [11] for the steady Stokes problem, where the DD
 50 method is based on a penalty term on the interface (in that case the Robin conditions
 51 are not equivalent to the physical ones). The convergence is shown for a modified
 52 pressure in the two-subdomains case. This issue of pressure converging up to a con-
 53 stant that depends on the subdomains is also raised in [33, 23] for the discrete Schwarz
 54 algorithm with a DDFV scheme applied to the semi-discrete in time Navier-Stokes
 55 system. In [12, 6], an optimized Schwarz DD method is studied, and applied at each
 56 time step to the semi-discrete in time Navier-Stokes equations. Other transmission
 57 conditions (Dirichlet / Neumann) are considered e.g. in [46, 21, 44, 49] for Stokes and
 58 Navier-Stokes equations.

59 In this article we consider global-in-time Schwarz methods which use waveform
 60 relaxation techniques, i.e. Schwarz waveform relaxation (SWR). Such iterative meth-
 61 ods use computations in the subdomains over the whole time interval, exchanging
 62 space-time boundary data through transmission conditions on the space-time inter-
 63 faces. The main advantage is that space-time discretizations can be chosen indepen-
 64 dently on each subdomain, and, at the end of each iteration, only a small amount of
 65 information is exchanged, which makes the parallelization (in space and time) very
 66 efficient.

67 The space-time boundary data play an important role in the convergence process
 68 and can be of Dirichlet [20, 22], absorbing, Robin (or Ventcell) type [19, 35, 4, 25, 24].
 69 The value of the Robin (or Ventcell) parameters can be optimized to improve conver-
 70 gence rates (see [19, 30, 35, 32]), and the corresponding method is called optimized
 71 Schwarz waveform relaxation (OSWR). This method is widely used and analyzed for
 72 fluid dynamics, see references above, and e.g. [35, 18, 36, 3, 5, 28, 1, 48].

73 For the application of the SWR method on the Navier-Stokes equations, we are
 74 aware of the article [3] where an OSWR method is proposed for the rotating 3D
 75 incompressible hydrostatic Navier-Stokes equations with free surface. However, the
 76 hydrostatic nature of the model modifies the structure of the continuity equation which
 77 now involves a transport term for the free surface (which plays the same role as the
 78 pressure in the momentum equation of the standard Navier-Stokes system), so that
 79 the results in [3] cannot apply to the problem considered in the present work. In [12],
 80 an SWR method for the Oseen equations is studied; optimal transparent boundary
 81 conditions are derived, and local approximations for these nonlocal conditions are
 82 proposed. No general convergence analysis of the resulting algorithm (e.g. via energy
 83 estimates) is given. A convergence factor is obtained in the idealized case of two
 84 half-space subdomains and unbounded time interval, via Laplace-Fourier transforms.

85 Concerning the compressible Euler and Navier-Stokes equations, in [14, 13] an
 86 SWR method is proposed and various numerical experiments are shown.

87 However, until now, there exists no convergence proof (for SWR or OSWR) for the
 88 incompressible Navier-Stokes equations. We contribute to the understanding of the
 89 behaviour of the OSWR method by attacking representative, though simpler, model
 90 problems. To begin with, we analyze the method on the evolutionary Stokes equations,

91 a simplified version of the evolutionary Navier-Stokes system in which the convection
 92 is simply discarded. The convergence analysis of the velocity iterates involved in the
 93 OSWR method, for the Stokes equations, can be performed in a similar manner as for
 94 parabolic equations. An extension of this analysis to the evolutionary Oseen equations
 95 (a linearization of the Navier-Stokes equations in which the convective velocity field
 96 is considered as a given datum) is given in [9]. However, the convergence analysis of
 97 the OSWR method has its own obstacle related to the pressure converging only up
 98 to constants in the various subdomains, as discussed above. A second purpose of this
 99 article is to propose a new technique, in the multidomain case, to recover the pressure
 100 from the velocity (at any iteration).

101 A third purpose of this article is to discuss the choice of the Robin parameters,
 102 which play a crucial role in the optimization of the convergence rate. Until recently,
 103 the common practice was to derive and optimize a convergence rate in the idealized
 104 case of two half-space subdomains and unbounded time interval, via Laplace-Fourier
 105 transforms performed on the continuous model (i.e. without taking into account the
 106 actual discretization method). We first follow this standard approach in this work,
 107 but in a second step modify it to also include the effect of the discretization in the
 108 time direction; the Robin parameters obtained with such a modification improve the
 109 convergence rate over the standard choice in our numerical tests. Note that studying
 110 the influence of the numerical scheme over the OSWR convergence rate is a recent
 111 approach, pursued for example in [15, 26, 2].

112 The remainder of this article is organized as follows. In section 2, we present
 113 the model problem and its multidomain form. Since the multi-domain formulation
 114 involves local Stokes problems with Robin boundary conditions, we prove the well-
 115 posedness of such problems in Section 3. Next, section 4 is dedicated to the algorithm.
 116 In section 5 we show that, in general, the pressure calculated by the OSWR algorithm
 117 will not converge to the monodomain solution. In section 6, we obtain a convergence
 118 result on the velocity through an energy estimate, and in section 7, we propose an
 119 astute technique to recover the pressure from the velocity. In section 8, a Fourier
 120 analysis is done to get a formulation for the convergence factor of the OSWR algo-
 121 rithm. In section 9, an optimization procedure (based on the convergence factor of the
 122 method), that allows to obtain efficient Robin parameters, is given. Then, numerical
 123 illustrations for the unsteady Stokes system follow in section 10.

124 **2. Presentation of the model and multidomain formulation.** For a bounded do-
 125 main $\Omega \subseteq \mathbb{R}^2$, and for a given viscosity coefficient $\nu > 0$ that we suppose constant and
 126 uniform, for given initial condition \mathbf{u}_0 and source term \mathbf{f} , we denote respectively by
 127 \mathbf{u} , p the velocity and pressure unknowns in the incompressible non-stationary Stokes
 128 system:

$$\begin{aligned}
 \partial_t \mathbf{u} - \nu \Delta \mathbf{u} + \nabla p &= \mathbf{f} & \text{in } & \Omega \times (0, T), \\
 \nabla \cdot \mathbf{u} &= 0 & \text{in } & \Omega \times (0, T), \\
 \mathbf{u}(\cdot, t = 0) &= \mathbf{u}_0 & \text{in } & \Omega, \\
 \mathbf{u} &= 0 & \text{on } & \partial\Omega \times (0, T).
 \end{aligned} \tag{2.1}$$

131 This system does not have a unique solution: if (\mathbf{u}, p) is a solution, then $(\mathbf{u}, p + c)$ is
 132 also a solution, for any constant c . Then, for uniqueness, one needs, for example, the
 133 zero-mean condition on the pressure

$$\int_{\Omega} p = 0. \tag{2.2}$$

136 Thus, we introduce the notation $L_0^2(\Omega) = \{p \in L^2(\Omega), \int_{\Omega} p = 0\}$.

137

138 Next, we shall introduce the following spaces, which are the completions, in $H^1(\Omega)$
 139 and in $L^2(\Omega)$, respectively, of the set of compactly supported C^∞ functions with
 140 vanishing divergence:

$$\begin{aligned} 141 \quad V &= \left\{ \mathbf{u} \in [H_0^1(\Omega)]^2, \nabla \cdot \mathbf{u} = 0 \right\}, \\ 142 \quad H &= \left\{ \mathbf{u} \in [L^2(\Omega)]^2, \nabla \cdot \mathbf{u} = 0, \mathbf{u} \cdot \mathbf{n}_{\partial\Omega} = 0 \text{ on } \partial\Omega \right\}, \end{aligned}$$

143 where $\mathbf{n}_{\partial\Omega}$ is the unit, outward pointing, normal vector field on $\partial\Omega$. We denote by V'
 144 the dual space of V . We recall ([7, Proposition IV.5.13]) that, if Ω , \mathbf{f} and \mathbf{u}_0 regular
 145 enough, problem (2.1)-(2.2) has a unique solution such that

$$\begin{aligned} 146 \quad \mathbf{u} &\in (L^2((0, T), V) \cap C^0([0, T], H)), \quad \partial_t \mathbf{u} \in L^2((0, T), V'), \\ 147 \quad p &\in W^{-1, \infty}((0, T), L_0^2(\Omega)). \end{aligned}$$

148 In order to apply a domain-decomposition strategy for this problem, we decompose Ω
 149 into M non-overlapping subdomains Ω_i , i.e. $\Omega_i \cap \Omega_j = \emptyset$ for $i \neq j$, and $\Omega = \bigcup_{i=1}^M \Omega_i$.
 150 For $i = 1, 2, \dots, M$, we denote by \mathcal{I}_i the set of indices of the neighbouring subdo-
 151 main(s) of Ω_i : it holds that $j \in \mathcal{I}_i$ if and only if $|\partial\Omega_i \cap \partial\Omega_j| > 0$, where $|\cdot|$ denotes
 152 the one dimensional measure. We denote by Γ_{ij} the interface (if it exists) between
 153 Ω_i and Ω_j , \mathbf{n}_{ij} the unit normal vector on Γ_{ij} , directed from Ω_i to Ω_j . Note that this
 154 implies that $\mathbf{n}_{ij} = -\mathbf{n}_{ji}$.

155

156 Denoting by \mathbf{u}_i , $(\mathbf{u}_0)_i$, p_i and \mathbf{f}_i the respective restrictions of \mathbf{u} , \mathbf{u}_0 , p and \mathbf{f} to Ω_i ,
 157 the monodomain problem is equivalent to the following multidomain one

$$\begin{aligned} 158 \quad \partial_t \mathbf{u}_i - \nu \Delta \mathbf{u}_i + \nabla p_i &= \mathbf{f}_i & \text{in } & \Omega_i \times (0, T), \\ & \nabla \cdot \mathbf{u}_i = 0 & \text{in } & \Omega_i \times (0, T), \\ & \mathbf{u}_i(\cdot, t = 0) = (\mathbf{u}_0)_i & \text{in } & \Omega_i, \\ 159 \quad & \mathbf{u}_i = 0 & \text{on } & (\partial\Omega \cap \partial\Omega_i) \times (0, T), \end{aligned} \quad (2.3)$$

160 for all $i \in \llbracket 1, M \rrbracket$, together with the physical transmission conditions on the space-time
 161 interfaces $\Gamma_{ij} \times (0, T)$, $j \in \mathcal{I}_i$, $i \in \llbracket 1, M \rrbracket$,

$$\begin{aligned} & \mathbf{u}_{ij} \cdot \mathbf{n}_{ij} = -\mathbf{u}_{ji} \cdot \mathbf{n}_{ji}, \\ & \mathbf{u}_j \times \mathbf{n}_{ij} = -\mathbf{u}_j \times \mathbf{n}_{ji}, \\ 162 \quad & \nu \partial_{\mathbf{n}_{ij}} \mathbf{u}_i \cdot \mathbf{n}_{ij} - p_i = \nu \partial_{\mathbf{n}_{ji}} \mathbf{u}_j \cdot \mathbf{n}_{ji} - p_j, \\ 163 \quad & \nu \partial_{\mathbf{n}_{ij}} \mathbf{u}_i \times \mathbf{n}_{ij} = \nu \partial_{\mathbf{n}_{ji}} \mathbf{u}_j \times \mathbf{n}_{ji}. \end{aligned} \quad (2.4)$$

164 For any choice of $(\alpha_{ij}, \alpha_{ji}, \beta_{ij}, \beta_{ji}) \in (\mathbb{R}^{+*})^4$, those conditions are equivalent to the
 165 following Robin transmission conditions on $\Gamma_{ij} \times (0, T) = \Gamma_{ji} \times (0, T)$:

$$\begin{aligned} & \alpha_{ij}(\nu \partial_{\mathbf{n}_{ij}} \mathbf{u}_i \cdot \mathbf{n}_{ij} - p_i) + \mathbf{u}_i \cdot \mathbf{n}_{ij} = \alpha_{ij}(\nu \partial_{\mathbf{n}_{ij}} \mathbf{u}_j \cdot \mathbf{n}_{ij} - p_j) + \mathbf{u}_j \cdot \mathbf{n}_{ij}, \\ 166 \quad & \alpha_{ji}(\nu \partial_{\mathbf{n}_{ji}} \mathbf{u}_j \cdot \mathbf{n}_{ji} - p_j) + \mathbf{u}_j \cdot \mathbf{n}_{ji} = \alpha_{ji}(\nu \partial_{\mathbf{n}_{ji}} \mathbf{u}_i \cdot \mathbf{n}_{ji} - p_i) + \mathbf{u}_i \cdot \mathbf{n}_{ji}, \\ & \beta_{ij} \nu \partial_{\mathbf{n}_{ij}} \mathbf{u}_i \times \mathbf{n}_{ij} + \mathbf{u}_i \times \mathbf{n}_{ij} = \beta_{ij} \nu \partial_{\mathbf{n}_{ij}} \mathbf{u}_j \times \mathbf{n}_{ij} + \mathbf{u}_j \times \mathbf{n}_{ij}, \\ 167 \quad & \beta_{ji} \nu \partial_{\mathbf{n}_{ji}} \mathbf{u}_j \times \mathbf{n}_{ji} + \mathbf{u}_j \times \mathbf{n}_{ji} = \beta_{ji} \nu \partial_{\mathbf{n}_{ji}} \mathbf{u}_i \times \mathbf{n}_{ji} + \mathbf{u}_i \times \mathbf{n}_{ji}. \end{aligned} \quad (2.5)$$

168 Finally, the zero-mean condition for the pressure is equivalent to

$$169 \quad \sum_{i=1}^M \int_{\Omega_i} p_i = 0. \quad (2.6)$$

170
171 This setting requires that we should study the Stokes system in a domain where
172 Robin boundary conditions are applied on a part of the boundary. This is what is
173 done in the next section.

174 **3. The Stokes problem with Robin boundary conditions.** We now consider a do-
175 main, still denoted by Ω , for which the boundary is decomposed into two parts:
176 $\partial\Omega = \Gamma_D \cup \Gamma_R$, with $|\Gamma_R| > 0$. Let \mathbf{n} be the outgoing normal vector on Γ_R ; we
177 consider the following system, with $\alpha > 0$ and $\beta > 0$

$$178 \quad \begin{aligned} \partial_t \mathbf{u} - \nu \Delta \mathbf{u} + \nabla p &= \mathbf{f} & \text{in } & \Omega \times (0, T), \\ \nabla \cdot \mathbf{u} &= 0 & \text{in } & \Omega \times (0, T), \\ \mathbf{u}(\cdot, t = 0) &= \mathbf{u}_0 & \text{in } & \Omega, \\ \mathbf{u} &= 0 & \text{on } & \Gamma_D \times (0, T), \\ \alpha(\nu \partial_{\mathbf{n}} \mathbf{u} \cdot \mathbf{n} - p) + \mathbf{u} \cdot \mathbf{n} &= g & \text{on } & \Gamma_R \times (0, T), \\ \beta \nu \partial_{\mathbf{n}} \mathbf{u} \times \mathbf{n} + \mathbf{u} \times \mathbf{n} &= \xi & \text{on } & \Gamma_R \times (0, T), \end{aligned} \quad (3.1)$$

179
180 where \mathbf{f} is at least in $[L^2(\Omega \times (0, T))]^2$, g and ξ are at least in $[L^2(\Gamma_R \times (0, T))]$.
181 In order to set this problem under an appropriate (parabolic) variational form, we
182 multiply the first equation by a divergence-free test function \mathbf{v} (smooth enough) that
183 vanishes on Γ_D and integrate by parts on Ω . The flux $(-\nu \partial_{\mathbf{n}} \mathbf{u} + p \mathbf{n})$ is then decom-
184 posed into normal and tangential parts and boundary conditions of (3.1) are used.
185 We obtain then the following parabolic variational problem

$$186 \quad \langle \partial_t \mathbf{u}, \mathbf{v} \rangle_{V'_D, V_D} + a(t, \mathbf{u}, \mathbf{v}) = c(t, \mathbf{v}), \quad \text{a.e. } t \in (0, T), \forall \mathbf{v} \in V_D, \quad (3.2)$$

$$187 \quad \mathbf{u}(0) = \mathbf{u}_0, \quad (3.3)$$

189 where the spaces are defined as

$$190 \quad V_D = \left\{ \mathbf{u} \in [H^1(\Omega)]^2, \mathbf{u} = 0 \text{ on } \Gamma_D, \nabla \cdot \mathbf{u} = 0 \right\},$$

$$191 \quad H_D = \left\{ \mathbf{u} \in [L^2(\Omega)]^2, \mathbf{u} \cdot \mathbf{n} = 0 \text{ on } \Gamma_D, \nabla \cdot \mathbf{u} = 0 \right\},$$

192 together with their linear and bilinear forms

$$193 \quad a(\mathbf{u}, \mathbf{v}) = \nu (\nabla \mathbf{u}, \nabla \mathbf{v})_{\Omega} + \frac{1}{\alpha} (\mathbf{u} \cdot \mathbf{n}, \mathbf{v} \cdot \mathbf{n})_{\Gamma_R} + \frac{1}{\beta} (\mathbf{u} \times \mathbf{n}, \mathbf{v} \times \mathbf{n})_{\Gamma_R}, \quad (3.4)$$

$$194 \quad c(t, \mathbf{v}) = (\mathbf{f}(t), \mathbf{v})_{\Omega} + \frac{1}{\alpha} (g(t), \mathbf{v} \cdot \mathbf{n})_{\Gamma_R} + \frac{1}{\beta} (\xi(t), \mathbf{v} \times \mathbf{n})_{\Gamma_R}. \quad (3.5)$$

196 Here, $(\cdot, \cdot)_D$ denotes, for any set D (whatever the space-dimension of D) the standard
197 scalar or the matrix-valued scalar L^2 product on D . In the same way, we shall use
198 the notation $\|\cdot\|_D$ for the associated $L^2(D)$ norm. All terms in the definition of the
199 forms a and c are well-defined for $(\mathbf{u}, \mathbf{v}) \in V_D \times V_D$.

200 From these definitions, V_D is dense in H_D and the embedding $V_D \subset H_D$ is
201 continuous. We can identify H_D with its dual space, and we are in the situation
202 where $V_D \subset H_D \equiv H'_D \subset V'_D$, which is the classical setting for parabolic equations
203 (see e.g. [17, Section 6.1], [8, Page 218]). In this context, we recall the following
204 theorem.

205 THEOREM 3.1. *Problem (3.2)-(3.3) admits a unique solution*

$$206 \quad \mathbf{u} \in (L^2((0, T), V_D) \cap C^0([0, T], H_D)),$$

207 with $\partial_t \mathbf{u} \in L^2((0, T), V'_D)$ if the following properties are verified

- 208 • $\mathbf{u}_0 \in H_D$ and $c \in L^2((0, T), V'_D)$,
- 209 • The function $t \mapsto a(t, \mathbf{u}, \mathbf{v})$ is measurable for all $(\mathbf{u}, \mathbf{v}) \in V_D^2$,
- 210 • $\exists M \in \mathbb{R}$ such that $|a(t, \mathbf{u}, \mathbf{v})| \leq M \|\mathbf{u}\|_{V_D} \|\mathbf{v}\|_{V_D}$ for almost every t and for all
- 211 $(\mathbf{u}, \mathbf{v}) \in V_D^2$,
- 212 • $\exists m > 0$ such that $a(t, \mathbf{u}, \mathbf{u}) \geq m \|\mathbf{u}\|_{V_D}^2$ for almost every t and for all $\mathbf{u} \in V_D$.

213 We shall apply this result to our setting, with the simplification that the bilinear form
214 defined by (3.4) does not depend on time. We obtain the following result:

215 THEOREM 3.2. *Assume that $\mathbf{f} \in L^2((0, T), [L^2(\Omega)]^2)$, $g, \xi \in L^2((0, T), L^2(\Gamma_R))$,
216 and $\mathbf{u}_0 \in H_D$. Let a and c be defined by (3.4) and (3.5), respectively. Then, problem
217 (3.2)–(3.3) admits a unique solution $\mathbf{u} \in (L^2((0, T), V_D) \cap C^0([0, T], H_D))$, which is
218 such that $\partial_t \mathbf{u} \in L^2((0, T), V'_D)$.*

219 *Proof.* We shall show that a and c verify the hypothesis of Theorem 3.1. First, it
220 is well-known that, as soon as $|\Gamma_R| > 0$, then

$$221 \quad \|\mathbf{u}\|_{V_D} := (\|\nabla \mathbf{u}\|_{\Omega}^2 + \|\mathbf{u}\|_{\Gamma_R}^2)^{\frac{1}{2}} = (\|\nabla \mathbf{u}\|_{\Omega}^2 + \|\mathbf{u} \cdot \mathbf{n}\|_{\Gamma_R}^2 + \|\mathbf{u} \times \mathbf{n}\|_{\Gamma_R}^2)^{\frac{1}{2}}$$

223 is a norm equivalent to the H^1 norm on V_D , and we shall therefore work with this
224 norm.

225 Let $M = \max\left(\nu, \frac{1}{\alpha}, \frac{1}{\beta}\right)$. From the Cauchy-Schwarz inequality, we get the con-
226 tinuity of $a(\cdot, \cdot)$:

$$227 \quad |a(\mathbf{u}, \mathbf{v})| \leq M \|\mathbf{u}\|_{V_D} \|\mathbf{v}\|_{V_D}, \quad \forall \mathbf{u}, \mathbf{v} \in V_D.$$

229 Let $m = \min\left(\nu, \frac{1}{\alpha}, \frac{1}{\beta}\right) > 0$. From the definition of $\|\cdot\|_{V_D}$, we get the coercivity
230 of $a(\cdot, \cdot)$:

$$231 \quad a(\mathbf{u}, \mathbf{u}) \geq m \|\mathbf{u}\|_{V_D}^2, \quad \forall \mathbf{u} \in V_D.$$

233 Then, for a.e. $t \in (0, T)$, the continuity of $c(t, \cdot)$ is deduced from the Cauchy-Schwarz
234 inequality and the equivalence between the $H^1(\Omega)$ -norm and $\|\cdot\|_{V_D}$:

$$235 \quad |c(t, \mathbf{v})| \leq \left[C_1 \|\mathbf{f}(t)\|_{\Omega} + \frac{1}{\alpha} \|g(t)\|_{\Gamma_R} + \frac{1}{\beta} \|\xi(t)\|_{\Gamma_R} \right] \|\mathbf{v}\|_{V_D}.$$

Moreover, thanks to the hypothesis on the time dependence of \mathbf{f} , g and ξ , the quantity

$$C_1 \|\mathbf{f}(t)\|_{\Omega} + \frac{1}{\alpha} \|g(t)\|_{\Gamma_R} + \frac{1}{\beta} \|\xi(t)\|_{\Gamma_R}$$

237 is square integrable on $(0, T)$, and we can now apply Theorem 3.1, which finishes the
238 proof. \square

Remark 3.3. Since V_D is continuously and densely embedded in H_D , the fact that
 $\mathbf{u} \in C^0([0, T], H_D)$ is a consequence of the fact that the space

$$\mathcal{W}(V_D, V'_D) := \{\mathbf{v} : (0, T) \mapsto V_D; \mathbf{v} \in L^2((0, T), V_D); \partial_t \mathbf{v} \in L^2((0, T), V'_D)\}$$

239 is included in $\mathcal{C}^0([0, T], H_D)$, as stated, for example, by [17, Lemma 6.2] and [7,
240 Theorem II.5.13].

241 This has the important implication that it is legitimate to consider $\mathbf{u}(t) \in H_D$ for
242 all $t \in [0, T]$. Moreover, the following integral equality holds for all $t \in [0, T]$ and for
243 all $(\mathbf{u}, \mathbf{v}) \in [\mathcal{W}(V_D, V'_D)]^2$ (see [17, Lemma 6.3] and [7, Theorem II.5.12]):

$$\int_0^t (\langle \partial_t \mathbf{u}(s), \mathbf{v}(s) \rangle_{V'_D, V_D} + \langle \partial_t \mathbf{v}(s), \mathbf{u}(s) \rangle_{V'_D, V_D}) ds = (\mathbf{u}(t), \mathbf{v}(t))_\Omega - (\mathbf{u}(0), \mathbf{v}(0))_\Omega. \quad (3.6)$$

244 Now, since we have obtained the velocity \mathbf{u} from the constrained variational problem (3.2)–(3.3), we shall construct the pressure by relaxing the divergence free condition on the velocity test functions, and we shall therefore consider the space

$$X_D = \left\{ \mathbf{v} \in [H^1(\Omega)]^2, \mathbf{v} = 0 \text{ on } \Gamma_D \right\},$$

245 equipped with the above-defined norm $\|\cdot\|_{V_D}$. Like often with the Stokes problem,
246 we shall rely on the surjectivity of the divergence operator, and on general properties
247 of surjective mappings in Hilbert spaces. More precisely, we shall use the following
248 results.

249 LEMMA 3.4. *The mapping B from X_D into $L^2(\Omega)$ defined by $B(\mathbf{v}) = -\nabla \cdot \mathbf{v}$ is
250 continuous and surjective.*

251 *Proof.* This is a special case of [17, Lemma 4.9] (with, using the notations of [17],
252 $\partial\Omega_1 = \Gamma_D$, $\partial\Omega_2 = \emptyset$, $\partial\Omega_3 = \emptyset$ and $\partial\Omega_4 = \Gamma_R$). \square

253 LEMMA 3.5. *Let L be in $\mathcal{L}(E; F)$ and L^T be its adjoint in $\mathcal{L}(F'; E')$, then if L is
254 surjective in F , then $\text{Im } L^T$ is closed in E' .*

255 Before stating the next Lemma, we recall the following definition (see, e.g. [7, Defini-
256 tion IV.2.1]) and properties (see, e.g. [7, Remark IV.2.1])

DEFINITION 3.6. *Let E be a Banach space with dual space E' ; then for any subset
 $A \subset E$, we define $A^\perp \subset E'$ as follows:*

$$A^\perp := \{\phi \in E', \forall x \in A, \langle \phi, x \rangle_{E', E} = 0\}$$

257 LEMMA 3.7. *If $A \subset C \subset E$, then $C^\perp \subset A^\perp$.*

258 LEMMA 3.8. *If A is a linear subspace of E , then $(A^\perp)^\perp = A$ if and only if A is
259 closed in E .*

260 Moreover, we also recall the following general result

261 LEMMA 3.9. *Let L be in $\mathcal{L}(E; F)$, then $(\text{Im } L^T)^\perp \subset \text{Ker } L$*

262 *Proof.* If $f \in (\text{Im } L^T)^\perp$, then $\langle L^T q, f \rangle_{E', E} = 0, \forall q \in F'$. Thus $\langle q, Lf \rangle_{F', F} = 0$
263 for all $q \in F'$, which means that $Lf = 0$, and thus $f \in \text{Ker } L$. \square

264 From these results, we obtain the following Lemma, which will be useful in the con-
265 struction of the pressure field:

266 LEMMA 3.10. *Let B^T be the adjoint operator of B , from $L^2(\Omega)$ into X'_D . Then
267 for any ℓ in X'_D that vanishes on V_D , there exists $P \in L^2(\Omega)$ such that $\ell = B^T P$.*

268 *Proof.* Since B is in $\mathcal{L}(X_D; L^2(\Omega))$ and is surjective (Lemma 3.4), then $(\text{Im } B^T)$
269 is closed in X'_D (Lemma 3.5), and $((\text{Im } B^T)^\perp)^\perp = \text{Im } B^T$ (Lemma 3.8). Now, using

270 Lemmas 3.9 and 3.7, we get $(\text{Ker } B)^\perp \subset ((\text{Im } B^T)^\perp)^\perp = \text{Im } B^T$. So if ℓ in X'_D
 271 vanishes on $V_D = \text{Ker } B$, then ℓ is in $(\text{Ker } B)^\perp$ and so in $\text{Im } B^T$, which exactly means
 272 that there exists $P \in L^2(\Omega)$ such that $\ell = B^T P$. \square

273 Using this result, we can now state the following theorem.

274 **THEOREM 3.11.** *Assume that $\mathbf{f} \in L^2((0, T), [L^2(\Omega)]^2)$, $\xi, g \in L^2((0, T), L^2(\Gamma_R))$
 275 and $\mathbf{u}_0 \in H_D$, then there exists unique $\mathbf{u} \in (L^2((0, T), V_D) \cap C^0([0, T], H_D))$ and
 276 $p \in W^{-1, \infty}((0, T), L^2(\Omega))$, with $\partial_t \mathbf{u} \in L^2((0, T), V'_D)$ such that (\mathbf{u}, p) verifies problem
 277 (3.1) in the sense that*

- 278 • \mathbf{u} verifies (3.2)–(3.3)
- 279 • $p = \partial_t P$ with $P \in L^\infty((0, T), L^2(\Omega))$ that satisfies

$$\int_0^t c(s, \mathbf{v}) ds - (\mathbf{u}(t), \mathbf{v})_\Omega + (\mathbf{u}_0, \mathbf{v})_\Omega - \int_0^t a(\mathbf{u}(s), \mathbf{v}) ds = - \int_\Omega P(t) \nabla \cdot \mathbf{v} \ , \ \forall \mathbf{v} \in X_D. \quad (3.7)$$

281 *Proof.* Let \mathbf{u} be the solution of (3.2)–(3.3), and consider, for this \mathbf{u} , the function
 282 $t \mapsto a(\mathbf{u}(t), \mathbf{v})$ and the function $t \mapsto c(t, \mathbf{v})$ where a and c are defined by (3.4) and (3.5).
 283 Then their definitions can be straightforwardly extended to consider $\mathbf{v} \in X_D$ and, for
 284 any $t \in (0, T)$, the following element of X'_D is well-defined:

$$b(t, \mathbf{v}) := \int_0^t c(s, \mathbf{v}) ds - (\mathbf{u}(t), \mathbf{v})_\Omega + (\mathbf{u}_0, \mathbf{v})_\Omega - \int_0^t a(\mathbf{u}(s), \mathbf{v}) ds \ , \ \forall \mathbf{v} \in X_D.$$

287 Indeed, one has that

$$\begin{aligned} \left| \int_0^t a(\mathbf{u}(s), \mathbf{v}) ds \right| &\leq \int_0^t M \|\mathbf{u}(s)\|_{X_D} \|\mathbf{v}\|_{X_D} ds \\ &\leq M \sqrt{t} \left[\int_0^t \|\mathbf{u}(s)\|_{X_D}^2 ds \right]^{\frac{1}{2}} \|\mathbf{v}\|_{X_D} \\ &\leq M \sqrt{T} \|\mathbf{u}\|_{L^2((0, T), V_D)} \|\mathbf{v}\|_{X_D}, \end{aligned}$$

292 and

$$\begin{aligned} \left| \int_0^t c(s, \mathbf{v}) ds \right| &\leq \int_0^t \left(C_1 \|\mathbf{f}(s)\|_\Omega + \frac{1}{\alpha} \|g(s)\|_{\Gamma_R} + \frac{1}{\beta} \|\xi(s)\|_{\Gamma_R} \right) \|\mathbf{v}\|_{X_D} \\ &\leq \gamma_1 \|\mathbf{v}\|_{X_D}, \end{aligned}$$

296 with

$$\gamma_1 = C_1 \sqrt{T} \|\mathbf{f}\|_{L^2((0, T), [L^2(\Omega)]^2)} + \frac{\sqrt{T}}{\alpha} \|g\|_{L^2((0, T), L^2(\Gamma_R))} + \frac{\sqrt{T}}{\beta} \|\xi\|_{L^2((0, T), L^2(\Gamma_R))}.$$

298 In addition, since \mathbf{u} belongs to $C^0([0, T], H_D)$, then

$$\begin{aligned} |-(\mathbf{u}(t), \mathbf{v})_\Omega + (\mathbf{u}_0, \mathbf{v})_\Omega| &\leq 2 \|\mathbf{u}\|_{L^\infty([0, T], [L^2(\Omega)]^2)} \|\mathbf{v}\|_\Omega \\ &\leq 2C_1 \|\mathbf{u}\|_{L^\infty([0, T], [L^2(\Omega)]^2)} \|\mathbf{v}\|_{X_D}. \end{aligned}$$

302 This leads to the fact that

$$|b(t, \mathbf{v})| \leq C_2 \|\mathbf{v}\|_{X_D}, \quad \forall \mathbf{v} \in V_D, \ \forall t \in (0, T), \quad (3.8)$$

with

$$C_2 = 2C_1 \|\mathbf{u}\|_{L^\infty([0,T],[L^2(\Omega)]^2)} + \gamma_1 + M\sqrt{T} \|\mathbf{u}\|_{L^2(0,T,V_D)}.$$

304 Moreover, from (3.2) and (3.6) (with \mathbf{v} not depending on time), we obtain that
 305 $b(t, \mathbf{v}) = 0$ for all $\mathbf{v} \in V_D$, for all $t \in (0, T)$. Thus, using Lemma 3.10, we conclude
 306 that, for all $t \in (0, T)$, there exists $P(t) \in L^2(\Omega)$ satisfying

$$307 \quad b(t, \mathbf{v}) = \langle B^T P(t), \mathbf{v} \rangle_{X'_D, X_D} = -(P(t), \nabla \cdot \mathbf{v})_\Omega = - \int_\Omega P(t) \nabla \cdot \mathbf{v} \, , \quad \forall \mathbf{v} \in X_D. \quad (3.9)$$

308 Moreover, the surjectivity of the divergence mapping leads to the following inf-sup
 309 condition: there exists $\gamma_2 > 0$, s.t.

$$310 \quad \inf_{q \in L^2(\Omega)} \sup_{\mathbf{v} \in X_D} \frac{(B\mathbf{v}, q)_\Omega}{\|\mathbf{v}\|_{X_D} \|q\|_{L^2(\Omega)}} = \gamma_2 > 0,$$

312 which implies, for all $q \in L^2(\Omega)$

$$313 \quad \gamma_2 \|q\|_{L^2(\Omega)} \leq \sup_{\mathbf{v} \in X_D} \frac{(B\mathbf{v}, q)_\Omega}{\|\mathbf{v}\|_{X_D}}. \quad (3.10)$$

315 In order to use $q = P(t)$ in (3.10), we need to evaluate $(B\mathbf{v}, P(t))_\Omega$. From (3.9), we
 316 obtain that $(B\mathbf{v}, P(t))_\Omega = \langle B^T P(t), \mathbf{v} \rangle_{X'_D, X_D} = b(t, \mathbf{v})$; together with (3.8), we get

$$317 \quad \|P(t)\|_{L^2(\Omega)} \leq \frac{1}{\gamma_2} \sup_{\mathbf{v} \in X_D} \frac{b(t, \mathbf{v})}{\|\mathbf{v}\|_{X_D}} \leq \frac{C_2}{\gamma_2}.$$

319 We conclude that $P(t) \in L^\infty((0, T), L^2(\Omega))$. Then, we define the pressure $p = \partial_t P$
 320 and thus $p \in H^{-1, \infty}((0, T), L^2(\Omega))$.

321 It remains to show that p is unique. Consider the case $\mathbf{u}_0 = 0$ and $c = 0$. Then,
 322 we have $\mathbf{u} = 0$, and (3.7) leads to $\int_\Omega P(t) \nabla \cdot \mathbf{v} = 0, \forall \mathbf{v} \in X_D$. From the surjectivity of
 323 the divergence mapping, one gets that $P(t) = 0$ for all t , and then $p = 0$. \square

324 **4. Optimized Schwarz Waveform Relaxation Algorithm.** The OSWR algorithm
 325 for solving the multidomain problem (2.3)–(2.4) is as follows.

Algorithm 4.1 (OSWR)

Choose initial Robin data g_{ij}^0, ξ_{ij}^0 on $\Gamma_{ij} \times (0, T)$, $j \in \mathcal{I}_i, i = 1, 2, \dots, M$

for $\ell = 1, 2, \dots$ **do**

1. Solve the local space-time Robin problems, for $i = 1, 2, \dots, M$

$$\begin{aligned} \partial_t \mathbf{u}_i^\ell - \nu \Delta \mathbf{u}_i^\ell + \nabla p_i^\ell &= \mathbf{f}_i & \text{in } & \Omega_i \times (0, T) \\ \nabla \cdot \mathbf{u}_i^\ell &= 0 & \text{in } & \Omega_i \times (0, T) \\ \mathbf{u}_i^\ell(\cdot, t=0) &= \mathbf{u}_{0,i} & \text{in } & \Omega_i \\ \alpha_{ij}(\nu \partial_{\mathbf{n}_{ij}} \mathbf{u}_i^\ell \cdot \mathbf{n}_{ij} - p_i^\ell) + \mathbf{u}_i^\ell \cdot \mathbf{n}_{ij} &= g_{ij}^{\ell-1} & \text{on } & \Gamma_{ij} \times (0, T), \quad j \in \mathcal{I}_i \\ \beta_{ij} \nu \partial_{\mathbf{n}_{ij}} \mathbf{u}_i^\ell \times \mathbf{n}_{ij} + \mathbf{u}_i^\ell \times \mathbf{n}_{ij} &= \xi_{ij}^{\ell-1} & \text{on } & \Gamma_{ij} \times (0, T), \quad j \in \mathcal{I}_i \\ \mathbf{u}_i^\ell &= 0 & \text{on } & (\partial\Omega_i \cap \partial\Omega) \times (0, T) \end{aligned} \quad (4.1)$$

2. Update the Robin terms $g_{ij}^\ell, \xi_{ij}^\ell$ on $\Gamma_{ij} \times (0, T)$, for $j \in \mathcal{I}_i, i = 1, 2, \dots, M$

$$g_{ij}^\ell = \alpha_{ij}(\nu \partial_{\mathbf{n}_{ij}} \mathbf{u}_j^\ell \cdot \mathbf{n}_{ij} - p_j^\ell) + \mathbf{u}_j^\ell \cdot \mathbf{n}_{ij}, \quad (4.2a)$$

$$\xi_{ij}^\ell = \beta_{ij} \nu \partial_{\mathbf{n}_{ij}} \mathbf{u}_j^\ell \times \mathbf{n}_{ij} + \mathbf{u}_j^\ell \times \mathbf{n}_{ij}. \quad (4.2b)$$

end for

326 *Remark 4.1.* Let $i \in \llbracket 1, M \rrbracket$, $j \in \mathcal{I}_i$. Formulas given by (4.2) can be rewritten as

$$327 \quad g_{ij}^\ell = \frac{\alpha_{ij}}{\alpha_{ji}} (\alpha_{ji} (\nu \partial_{\mathbf{n}_{ji}} \mathbf{u}_j^\ell \cdot \mathbf{n}_{ji} - p_j^\ell) + \mathbf{u}_j^\ell \cdot \mathbf{n}_{ji}) - \frac{\alpha_{ij}}{\alpha_{ji}} \mathbf{u}_j^\ell \cdot \mathbf{n}_{ji} + \mathbf{u}_j^\ell \cdot \mathbf{n}_{ij}$$

$$328 \quad \xi_{ij}^\ell = \frac{\beta_{ij}}{\beta_{ji}} (\beta_{ji} \nu \partial_{\mathbf{n}_{ji}} \mathbf{u}_j^\ell \times \mathbf{n}_{ji} + \mathbf{u}_j^\ell \times \mathbf{n}_{ji}) - \frac{\beta_{ij}}{\beta_{ji}} \mathbf{u}_j^\ell \times \mathbf{n}_{ji} + \mathbf{u}_j^\ell \times \mathbf{n}_{ij},$$

330 or equivalently, using the Robin transmission conditions in (4.1),

$$331 \quad g_{ij}^\ell = \frac{\alpha_{ij}}{\alpha_{ji}} g_{ji}^{\ell-1} - \frac{\alpha_{ij} + \alpha_{ji}}{\alpha_{ji}} \mathbf{u}_j^\ell \cdot \mathbf{n}_{ji}, \quad (4.3a)$$

$$332 \quad \xi_{ij}^\ell = \frac{\beta_{ij}}{\beta_{ji}} \xi_{ji}^{\ell-1} - \frac{\beta_{ij} + \beta_{ji}}{\beta_{ji}} \mathbf{u}_j^\ell \times \mathbf{n}_{ji}. \quad (4.3b)$$

334 One advantage of formula (4.3) is that, if $g_{ij}^{\ell-1}$ and $\xi_{ij}^{\ell-1}$ have $L^2(\Gamma_{ij})$ regularity,
 335 so will g_{ij}^ℓ and ξ_{ij}^ℓ . Indeed, in (4.3) the regularities of g_{ij}^ℓ and ξ_{ij}^ℓ depend only on
 336 those of $g_{ji}^{\ell-1}$, $\xi_{ji}^{\ell-1}$ and \mathbf{u}_j^ℓ , whose trace is in $L^2((0, T), H^{\frac{1}{2}}(\Gamma_{ij}))$ (recall that we have
 337 $\mathbf{u}_j^\ell \in L^2((0, T), [H^1(\Omega_j)]^2)$, see Section 3). On the other hand, formula (4.2) will
 338 return new Robin boundary data g_{ij}^ℓ and ξ_{ij}^ℓ with a lower regularity, which is not
 339 satisfying for an iterative algorithm. Another advantage of formula (4.3) is that it is
 340 easier to implement in practice, than formula (4.2).

341 Now, we may express the iterative algorithm in the following way. We first define

$$342 \quad V_i = \{ \mathbf{u} \in [H^1(\Omega_i)]^2, \mathbf{u} = 0 \text{ on } \partial\Omega_i \cap \partial\Omega, \nabla \cdot \mathbf{u} = 0 \text{ in } \Omega_i \},$$

$$343 \quad H_i = \{ \mathbf{u} \in [L^2(\Omega_i)]^2, \mathbf{u} \cdot \mathbf{n}_{\partial\Omega_i} = 0 \text{ on } \partial\Omega_i \cap \partial\Omega, \nabla \cdot \mathbf{u} = 0 \text{ in } \Omega_i \}.$$

$$344 \quad X_i = \left\{ \mathbf{u} \in [H^1(\Omega_i)]^2, \mathbf{u} = 0 \text{ on } \partial\Omega_i \cap \partial\Omega \right\},$$

345 Then, we set, for all $\mathbf{u}, \mathbf{v} \in X_i$ and $t \in (0, T)$,

$$a_i(\mathbf{u}, \mathbf{v}) := \nu (\nabla \mathbf{u}, \nabla \mathbf{v})_{\Omega_i} + \sum_{j \in \mathcal{I}_i} \frac{1}{\alpha_{ij}} (\mathbf{u} \cdot \mathbf{n}_{ij}, \mathbf{v} \cdot \mathbf{n}_{ij})_{\Gamma_{ij}} + \frac{1}{\beta_{ij}} (\mathbf{u} \times \mathbf{n}_{ij}, \mathbf{v} \times \mathbf{n}_{ij})_{\Gamma_{ij}},$$

$$346 \quad c_i^\ell(t, \mathbf{v}) := (\mathbf{f}(t), \mathbf{v})_{\Omega_i} + \sum_{j \in \mathcal{I}_i} \frac{1}{\alpha_{ij}} (g_{ij}^{\ell-1}(t), \mathbf{v} \cdot \mathbf{n}_{ij})_{\Gamma_{ij}} + \frac{1}{\beta_{ij}} (\xi_{ij}^{\ell-1}(t), \mathbf{v} \times \mathbf{n}_{ij})_{\Gamma_{ij}},$$

$$347 \quad (4.4)$$

348 and the algorithm reads: for all $\ell \geq 1$, given $g_{ij}^{\ell-1}, \xi_{ij}^{\ell-1}$ on each space-time interface
 349 $\Gamma_{ij} \times (0, T)$, solve, for each $i = 1 \dots M$:

$$350 \quad \langle \partial_t \mathbf{u}_i^\ell, \mathbf{v} \rangle_{V_i', V_i} + a_i(\mathbf{u}_i^\ell, \mathbf{v}) = c_i^\ell(t, \mathbf{v}), \quad \text{a.e. } t \in (0, T), \forall \mathbf{v} \in V_i, \quad (4.5)$$

$$351 \quad \mathbf{u}_i^\ell(0) = \mathbf{u}_{0,i}.$$

352 Then we construct $p_i^\ell = \partial_t P_i^\ell$, where P_i^ℓ is such that

$$353 \quad (\mathbf{u}_i^\ell(t), \mathbf{v})_{\Omega_i} - (\mathbf{u}_{0,i}, \mathbf{v})_{\Omega_i} + \int_0^t a_i(\mathbf{u}_i^\ell(s), \mathbf{v}) ds - (P_i^\ell, \nabla \cdot \mathbf{v})_{\Omega_i} - \int_0^t c_i^\ell(s, \mathbf{v}) ds = 0,$$

$$\forall \mathbf{v} \in X_i.$$

$$354 \quad (4.6)$$

355 Finally, the data are updated by using (4.3a)–(4.3b) on the space-time interfaces.

356 With this formulation, we can state the following result

357 THEOREM 4.2. Assume that $g_{ij}^0, \xi_{ij}^0 \in L^2((0, T), L^2(\Gamma_{ij}))$ and $\mathbf{u}_0|_{\Omega_i} \in H_i$. Then,
 358 the OSWR algorithm is well-defined and for all ℓ , $\mathbf{u}_i^\ell \in L^2((0, T), V_i) \cap C^0([0, T], H_i)$,
 359 $\partial_t \mathbf{u}_i^\ell \in L^2((0, T), V_i')$, $p_i^\ell \in W^{-1, \infty}((0, T), L^2(\Omega_i))$ and $g_{ij}^\ell, \xi_{ij}^\ell \in L^2((0, T), L^2(\Gamma_{ij}))$.

360 *Proof.* By Theorem 3.11, if $g_{ij}^{\ell-1}, \xi_{ij}^{\ell-1} \in L^2((0, T), L^2(\Gamma_{ij}))$, then one gets \mathbf{u}_i^ℓ
 361 verifying (4.5) with $\mathbf{u}_i^\ell \in L^2((0, T), V_i) \cap C^0([0, T], H_i)$ and $\partial_t \mathbf{u}_i^\ell \in L^2((0, T), V_i')$.
 362 Additionally, Theorem 3.11 tells us that there exists P_i^ℓ verifying (4.6). We take
 363 $p_i^\ell = \partial_t P_i^\ell \in W^{-1, \infty}((0, T), L^2(\Omega_i))$.

364 Using the trace theorem, the normal and tangent traces of \mathbf{u}_i^ℓ on $\Gamma_{ij} \times (0, T)$
 365 belong to $L^2((0, T), L^2(\Gamma_{ij}))$. Hence, using the update formula (4.3), we infer that
 366 $g_{ij}^\ell, \xi_{ij}^\ell \in L^2((0, T), L^2(\Gamma_{ij}))$.

367 The proof is then carried out by a simple induction. \square

368 *Remark 4.3.* The OSWR algorithm is constructed without considering the last
 369 condition (2.6), hence it may not converge to the monodomain solution. We shall show
 370 in the next section that, indeed, the pressure in each subdomain may not converge to
 371 the restriction of the monodomain pressure.

372 **5. First observations on the two subdomains case.** For the trivial case of a one-
 373 dimensional problem and two subdomains, one can show that the velocity iterates
 374 converge, while the pressure iterates do not converge in general, see [9].

375 This result generalizes to higher dimensions as follows : let us consider the two-
 376 subdomain case, i.e. $M = 2$. To simplify notation, we set $\Gamma := \Gamma_{12} = \Gamma_{21}$, and for
 377 any ϕ in (α, g, \mathbf{u}) , we write ϕ_1 and ϕ_2 instead of ϕ_{12} and ϕ_{21} , respectively.

378 The divergence-free condition of the velocity in each subdomain leads to

$$379 \int_{\partial\Omega_i} \mathbf{u}_i^\ell \cdot \mathbf{n}_{\partial\Omega_i} = 0 = \int_{\Gamma} \mathbf{u}_i^\ell \cdot \mathbf{n}_i, \quad i = 1, 2. \quad (5.1)$$

381 The update of Robin terms for the normal components can also be written as

$$382 g_i^\ell = \frac{\alpha_i}{\alpha_j} g_j^{\ell-1} - \frac{\alpha_i + \alpha_j}{\alpha_j} \mathbf{u}_j^\ell \cdot \mathbf{n}_j, \quad j = 3 - i, \quad i = 1, 2.$$

384 Integrating over Γ , and taking (5.1) into account, we get

$$385 \int_{\Gamma} g_i^\ell = \frac{\alpha_i}{\alpha_j} \int_{\Gamma} g_j^{\ell-1} = \int_{\Gamma} g_i^{\ell-2}, \quad j = 3 - i, \quad i = 1, 2.$$

387 Therefore, a necessary condition for the convergence of the algorithm to the mon-
 388 odomain solution is

$$389 \int_{\Gamma} g_i^0 = \int_{\Gamma} g_i, \quad i = 1, 2, \quad (5.2)$$

391 with $g_i = \alpha_i(\nu \partial_{\mathbf{n}_i} \mathbf{u} \cdot \mathbf{n}_i - p) + \mathbf{u} \cdot \mathbf{n}_i$, $i = 1, 2$, in which (\mathbf{u}, p) is the monodomain
 392 solution of problem (2.1). Condition (5.2) cannot be achieved in practice because the
 393 quantity g_i , $i = 1, 2$, is not known.

394 More precisely, whereas the convergence of the velocity iterates will be proven in
 395 Section 6 below, independently of condition (5.2), the pressure iterates will converge
 396 only if condition (5.2) is satisfied, and thus will not converge in general. A correction
 397 technique to recover the pressure from the velocity will be proposed in Section 7.

398 **6. Convergence of the velocity via energy estimate.** In this Section, we suppose
 399 additional regularity on \mathbf{u}_0 , \mathbf{f} and Ω , which leads to regularity properties of the strong
 400 solution of problem (2.1)–(2.2). Namely, we recall [31, Theorem 1, Page 86].

401 **THEOREM 6.1.** *Let Ω be a bounded domain of \mathbb{R}^2 with twice continuously differ-*
 402 *entiable boundary. For any $\mathbf{u}_0 \in V$ and $\mathbf{f} \in L^2((0, T), L^2(\Omega))^2$, problem (2.1)–(2.2)*
 403 *has a unique solution (\mathbf{u}, p) such that*

$$404 \quad \mathbf{u} \in C^0([0, T], V) \cap L^2((0, T), (H^2(\Omega))^2), \quad \partial_t \mathbf{u} \in L^2((0, T), L^2(\Omega))^2,$$

$$405 \quad p \in L^2((0, T), H^1(\Omega)).$$

406 Using Theorem 6.1, we prove that, if its hypotheses are satisfied, then the velocity
 407 iterates converge to the monodomain velocity.

408 **THEOREM 6.2.** *Assume that the hypotheses of Theorem 6.1 are satisfied. Let g_{ij}^0*
 409 *and ξ_{ij}^0 belong to $L^2((0, T), L^2(\Gamma_{ij}))$ and let \mathbf{u}_i^ℓ be the velocity component of the solution*
 410 *of Algorithm 4.1 (OSWR). Then, if $\alpha_{ij} = \alpha_{ji}$ and $\beta_{ij} = \beta_{ji}$, the sequence \mathbf{u}_i^ℓ converges*
 411 *to $\mathbf{u}_i = \mathbf{u}|_{\Omega_i}$ in $C^0([0, T], H_i) \cap L^2(0, T, V_i)$.*

412 *Proof.* Denote by $p_i = p|_{\Omega_i}$. Then, thanks to the extra regularity of (\mathbf{u}, p) given
 413 by Theorem 6.1, we can define its Robin trace on any space-time interface $\Gamma_{ij} \times (0, T)$
 414

$$415 \quad g_{ij}^\ell = \frac{\alpha_{ij}}{\alpha_{ji}} g_{ji}^{\ell-1} - \frac{\alpha_{ij} + \alpha_{ji}}{\alpha_{ji}} \mathbf{u}_j^\ell \cdot \mathbf{n}_{ji}, \quad (6.1a)$$

$$416 \quad \xi_{ij}^\ell = \frac{\beta_{ij}}{\beta_{ji}} \xi_{ji}^{\ell-1} - \frac{\beta_{ij} + \beta_{ji}}{\beta_{ji}} \mathbf{u}_j^\ell \times \mathbf{n}_{ji}. \quad (6.1b)$$

418 and they both belong to $L^2((0, T), L^2(\Gamma_{ij}))$. Then (2.5) implies

$$419 \quad g_{ij}^\ell = \frac{\alpha_{ij}}{\alpha_{ji}} g_{ji}^{\ell-1} - \frac{\alpha_{ij} + \alpha_{ji}}{\alpha_{ji}} \mathbf{u}_j^\ell \cdot \mathbf{n}_{ji}, \quad (6.2a)$$

$$420 \quad \xi_{ij}^\ell = \frac{\beta_{ij}}{\beta_{ji}} \xi_{ji}^{\ell-1} - \frac{\beta_{ij} + \beta_{ji}}{\beta_{ji}} \mathbf{u}_j^\ell \times \mathbf{n}_{ji}. \quad (6.2b)$$

422 Moreover, (\mathbf{u}_i, p_i) is the strong solution of each local Robin boundary problem with
 423 source term \mathbf{f}_i , initial condition $\mathbf{u}_{0,i}$ and Robin terms g_{ij} and ξ_{ij} on Γ_{ij} . We can write
 424 these local problems in variational forms similar to (4.4)–(4.5), in which we replace g_{ij}^ℓ
 425 by g_{ij} and ξ_{ij}^ℓ by ξ_{ij} .

426 We define the errors as the differences between the iterates and the restrictions
 427 (to each subdomain) of the monodomain solution and denote by

$$428 \quad \mathbf{e}_i^\ell := \mathbf{u}_i^\ell - \mathbf{u}_i, \quad h_{ij}^\ell = g_{ij}^\ell - g_{ij}, \quad \zeta_{ij}^\ell = \xi_{ij}^\ell - \xi_{ij}, \quad j \in \mathcal{I}_i, \quad i \in \llbracket 1, M \rrbracket. \quad (6.3)$$

429 Then, the errors also verify the following variational problems similar to (4.4)–(4.5):
 430 for a.e. $t \in (0, T)$, $\forall \mathbf{v} \in V_i$,

$$431 \quad \langle \partial_t \mathbf{e}_i^\ell, \mathbf{v} \rangle_{V_i', V_i} + a_i(\mathbf{e}_i^\ell, \mathbf{v}) = \sum_{j \in \mathcal{I}_i} \frac{1}{\alpha_{ij}} (h_{ij}^{\ell-1}, \mathbf{v} \cdot \mathbf{n}_{ij})_{\Gamma_{ij}} + \sum_{j \in \mathcal{I}_i} \frac{1}{\beta_{ij}} (\zeta_{ij}^{\ell-1}, \mathbf{v} \times \mathbf{n}_{ij})_{\Gamma_{ij}}, \quad (6.4)$$

432 with initial condition $\mathbf{e}_i^\ell(0) = 0$. All integrals on Γ_{ij} are well defined since g_{ij} and ξ_{ij}
 433 are both in $L^2((0, T), L^2(\Gamma_{ij}))$, and since we have proved that this is also the case
 434 for g_{ij}^ℓ and ξ_{ij}^ℓ as soon as it is true for $\ell = 0$.

435 With $\alpha_{ij} = \alpha_{ji}$ and $\beta_{ij} = \beta_{ji}$, the update formulas (4.3) and (6.2) for the Robin
436 terms on $\Gamma_{ij} \times (0, T)$ lead to

$$437 \quad \mathbf{e}_i^\ell \cdot \mathbf{n}_{ij} = \frac{1}{2} (h_{ij}^{\ell-1} - h_{ji}^\ell) \quad , \quad \mathbf{e}_i^\ell \times \mathbf{n}_{ij} = \frac{1}{2} (\zeta_{ij}^{\ell-1} - \zeta_{ji}^\ell) . \quad (6.5)$$

439 Choosing \mathbf{e}_i^ℓ as test function in (6.4), one gets

$$440 \quad \begin{aligned} & \langle \partial_t \mathbf{e}_i^\ell, \mathbf{e}_i^\ell \rangle_{V_i', V_i} + \nu (\nabla \mathbf{e}_i^\ell, \nabla \mathbf{e}_i^\ell)_{\Omega_i} \\ & + \sum_{j \in \mathcal{I}_i} \frac{1}{\alpha_{ij}} (\mathbf{e}_i^\ell \cdot \mathbf{n}_{ij}, \mathbf{e}_i^\ell \cdot \mathbf{n}_{ij})_{\Gamma_{ij}} + \sum_{j \in \mathcal{I}_i} \frac{1}{\beta_{ij}} (\mathbf{e}_i^\ell \times \mathbf{n}_{ij}, \mathbf{e}_i^\ell \times \mathbf{n}_{ij})_{\Gamma_{ij}} \\ & = \sum_{j \in \mathcal{I}_i} \frac{1}{\alpha_{ij}} (h_{ij}^{\ell-1}, \mathbf{e}_i^\ell \cdot \mathbf{n}_{ij})_{\Gamma_{ij}} + \sum_{j \in \mathcal{I}_i} \frac{1}{\beta_{ij}} (\zeta_{ij}^{\ell-1}, \mathbf{e}_i^\ell \times \mathbf{n}_{ij})_{\Gamma_{ij}} . \end{aligned} \quad (6.6)$$

442 On the boundary Γ_{ij} , $j \in \mathcal{I}_i$, replacing (6.5) into (6.6), one gets

$$443 \quad \begin{aligned} & \langle \partial_t \mathbf{e}_i^\ell, \mathbf{e}_i^\ell \rangle_{V_i', V_i} + \nu (\nabla \mathbf{e}_i^\ell, \nabla \mathbf{e}_i^\ell)_{\Omega_i} + \frac{1}{4} \sum_{j \in \mathcal{I}_i} \frac{1}{\alpha_{ij}} (h_{ij}^{\ell-1} - h_{ji}^\ell, h_{ij}^{\ell-1} - h_{ji}^\ell)_{\Gamma_{ij}} \\ & + \frac{1}{4} \sum_{j \in \mathcal{I}_i} \frac{1}{\beta_{ij}} (\zeta_{ij}^{\ell-1} - \zeta_{ji}^\ell, \zeta_{ij}^{\ell-1} - \zeta_{ji}^\ell)_{\Gamma_{ij}} \\ & = \frac{1}{2} \sum_{j \in \mathcal{I}_i} \frac{1}{\alpha_{ij}} (h_{ij}^{\ell-1}, h_{ij}^{\ell-1} - h_{ji}^\ell)_{\Gamma_{ij}} + \frac{1}{2} \sum_{j \in \mathcal{I}_i} \frac{1}{\beta_{ij}} (\zeta_{ij}^{\ell-1}, \zeta_{ij}^{\ell-1} - \zeta_{ji}^\ell)_{\Gamma_{ij}} , \end{aligned}$$

447 or equivalently

$$448 \quad \begin{aligned} & \langle \partial_t \mathbf{e}_i^\ell, \mathbf{e}_i^\ell \rangle_{V_i', V_i} + \nu \|\nabla \mathbf{e}_i^\ell\|_{\Omega_i}^2 + \frac{1}{4} \sum_{j \in \mathcal{I}_i} \frac{1}{\alpha_{ij}} \|h_{ji}^\ell\|_{\Gamma_{ij}}^2 + \frac{1}{4} \sum_{j \in \mathcal{I}_i} \frac{1}{\beta_{ij}} \|\zeta_{ji}^\ell\|_{\Gamma_{ij}}^2 \\ & = \frac{1}{4} \sum_{j \in \mathcal{I}_i} \frac{1}{\alpha_{ij}} \|h_{ij}^{\ell-1}\|_{\Gamma_{ij}}^2 + \frac{1}{4} \sum_{j \in \mathcal{I}_i} \frac{1}{\beta_{ij}} \|\zeta_{ij}^{\ell-1}\|_{\Gamma_{ij}}^2 , \end{aligned} \quad (6.7)$$

450 (recall that notation $\|\cdot\|_D$ corresponds to the $L^2(D)$ -norm for any set D).

451 Adapting (3.6) to Ω_i , integrating (6.7) on $(0, T)$, and using that $\mathbf{e}_i^\ell(0) = 0$, we get

$$452 \quad \begin{aligned} & \|\mathbf{e}_i^\ell(T)\|_{\Omega_i}^2 + 2\nu \int_0^T \|\nabla \mathbf{e}_i^\ell\|_{\Omega_i}^2 + \sum_{j \in \mathcal{I}_i} \frac{1}{2\alpha_{ij}} \int_0^T \|h_{ji}^\ell\|_{\Gamma_{ij}}^2 + \sum_{j \in \mathcal{I}_i} \frac{1}{2\beta_{ij}} \int_0^T \|\zeta_{ji}^\ell\|_{\Gamma_{ij}}^2 \\ & = \sum_{j \in \mathcal{I}_i} \frac{1}{2\alpha_{ij}} \int_0^T \|h_{ij}^{\ell-1}\|_{\Gamma_{ij}}^2 + \sum_{j \in \mathcal{I}_i} \int_0^T \frac{1}{2\beta_{ij}} \|\zeta_{ij}^{\ell-1}\|_{\Gamma_{ij}}^2 . \end{aligned} \quad (6.8)$$

454 Then, summing with respect to i , from 1 to M , we get

$$455 \quad \sum_{i=1}^M \|\mathbf{e}_i^\ell(\cdot, T)\|_{\Omega_i}^2 + 2\nu \sum_{i=1}^M \int_0^T \|\nabla \mathbf{e}_i^\ell\|_{\Omega_i}^2 + E_R^\ell = E_R^{\ell-1} ,$$

457 where $E_R^\ell = \sum_{i=1}^M \sum_{j \in \mathcal{I}_i} \frac{1}{2\beta_{ij}} \int_0^T \|\zeta_{ij}^\ell\|_{\Gamma_{ij}}^2 + \sum_{i=1}^M \sum_{j \in \mathcal{I}_i} \frac{1}{2\alpha_{ij}} \int_0^T \|h_{ij}^\ell\|_{\Gamma_{ij}}^2$.

458 Summing now with respect to ℓ , from 1 to L , we obtain

$$459 \quad \sum_{\ell=1}^L \sum_{i=1}^M \|\mathbf{e}_i^\ell(\cdot, T)\|_{\Omega_i}^2 + 2\nu \sum_{\ell=1}^L \sum_{i=1}^M \int_0^T \|\nabla \mathbf{e}_i^\ell\|_{\Omega_i}^2(t) dt + E_R^L = E_R^0 .$$

460

461 As $E_R^L \geq 0$ for all L , the sums $\sum_{\ell=1}^L \sum_{i=1}^M \|\mathbf{e}_i^\ell(\cdot, T)\|_{\Omega_i}^2$ and $\sum_{\ell=1}^L \sum_{i=1}^M \int_0^T \|\nabla \mathbf{e}_i^\ell\|_{\Omega_i}^2$
 462 are bounded; hence $\|\mathbf{e}_i^\ell(T)\|_{\Omega_i}^2$ and $\int_0^T \|\nabla \mathbf{e}_i^\ell\|_{\Omega_i}^2(t) dt$ tend to 0 when $\ell \rightarrow \infty$.
 463 In addition, in (6.8), we can integrate on $(0, t)$ instead of $(0, T)$, and we get for all
 464 $t \in (0, T)$

$$\sum_{\ell=1}^L \sum_{i=1}^M \|\mathbf{e}_i^\ell(t)\|_{\Omega_i}^2 \leq E_R^0.$$

465 This first leads to the convergence of $\|\mathbf{e}_i^\ell(t)\|_{\Omega_i}$ to 0 for all t and thus to the convergence
 466 of \mathbf{e}_i^ℓ to 0 in $\mathcal{C}^0([0, T], H_i)$, but also to the fact that, integrating on $(0, T)$, it holds
 467 that

$$\sum_{\ell=1}^L \sum_{i=1}^M \int_0^T \|\mathbf{e}_i^\ell(t)\|_{\Omega_i}^2 dt \leq T E_R^0.$$

472 This implies that $\int_0^T \|\mathbf{e}_i^\ell(t)\|_{\Omega_i}^2 dt$ tends to 0 when $\ell \rightarrow +\infty$. Then, summing with
 473 $\int_0^T \|\nabla \mathbf{e}_i^\ell\|_{\Omega_i}^2(t) dt$ that also tends to 0, we have that $\int_0^T \|\mathbf{e}_i^\ell(t)\|_{[H^1(\Omega_i)]^2}^2 dt$ tends to 0,
 474 or, in other words, that \mathbf{e}_i^ℓ tends to 0 in $L^2((0, T), V_i)$, for $i \in \llbracket 1, M \rrbracket$. \square

475 Now, we prove a convergence result for the pressure. We set $P(t) = \int_0^t p(s) ds$ and
 476 $P_i = P|_{\Omega_i}$ and denote the error by $D_i^\ell(t) = (P_i^\ell - P_i)(t)$, $i \in \llbracket 1, M \rrbracket$. Then we can
 477 state the following result.

478 **COROLLARY 6.3.** *Let all hypotheses of Theorem 6.2 be satisfied. Then for all*
 479 *$t \in [0, T]$ it holds that $\|D_i^\ell(t) - \frac{1}{|\Omega_i|} \int_{\Omega_i} D_i^\ell(t)\|_{\Omega_i} \rightarrow 0$ when $\ell \rightarrow \infty$.*

480 *Proof.* Let $i \in \llbracket 1, M \rrbracket$. As (\mathbf{u}_i, p_i) is the strong solution of the Robin problem
 481 with boundary conditions g_{ij} , ξ_{ij} , $j \in \mathcal{I}_i$, then P_i verifies a variational formulation
 482 similar to (4.6) : $\forall \mathbf{v} \in X_i$ it holds

$$483 \quad (\mathbf{u}_i(t), \mathbf{v})_{\Omega_i} - (\mathbf{u}_{0,i}, \mathbf{v})_{\Omega_i} + \int_0^t a_i(\mathbf{u}_i(s), \mathbf{v}) ds - (P_i(t), \nabla \cdot \mathbf{v})_{\Omega_i} - \int_0^t c_i(s, \mathbf{v}) ds = 0 \quad (6.9)$$

484 Then, from (4.6) and (6.9), taking the test function $\mathbf{v} \in [H_0^1(\Omega_i)]^2 \subset X_i$, the bound-
 485 ary terms in $c_i^\ell(s, \mathbf{v})$ and $c_i(s, \mathbf{v})$ vanish and then $c_i^\ell(s, \mathbf{v}) - c_i(s, \mathbf{v})$ also vanishes. Then
 486 we get

$$487 \quad (D_i^\ell(t), \nabla \cdot \mathbf{v})_{\Omega_i} = (\mathbf{e}_i^\ell(t), \mathbf{v})_{\Omega_i} + \int_0^t a_i(\mathbf{e}_i^\ell(s), \mathbf{v}) ds, \forall \mathbf{v} \in [H_0^1(\Omega_i)]^2.$$

489 As $(c, \nabla \cdot \mathbf{v})_{\Omega_i} = 0$ for all constants c and $\mathbf{v} \in [H_0^1(\Omega_i)]^2$, the above formulation
 490 implies that $\forall \mathbf{v} \in [H_0^1(\Omega_i)]^2$

$$491 \quad (D_i^\ell(t) - \frac{1}{|\Omega_i|} \int_{\Omega_i} D_i^\ell(t), \nabla \cdot \mathbf{v})_{\Omega_i} = (\mathbf{e}_i^\ell(t), \mathbf{v})_{\Omega_i} + \int_0^t a_i(\mathbf{e}_i^\ell(s), \mathbf{v}) ds.$$

493 Since $(D_i^\ell - \frac{1}{|\Omega_i|} \int_{\Omega_i} D_i^\ell) \in L_0^2(\Omega_i) = \{p \in L^2(\Omega_i), \int_{\Omega_i} p = 0\}$, $i \in \llbracket 1, M \rrbracket$, from the
 494 inf-sup condition there exists γ_3 s.t.

$$495 \quad \|D_i^\ell - \frac{1}{|\Omega_i|} \int_{\Omega_i} D_i^\ell\|_{\Omega_i} \leq \frac{1}{\gamma_3} \sup_{\mathbf{v} \in [H_0^1(\Omega_i)]^2} \frac{|(\mathbf{e}_i^\ell(t), \mathbf{v})_{\Omega_i} + \int_0^t a_i(\mathbf{e}_i^\ell(s), \mathbf{v}) ds|}{\|\mathbf{v}\|_{[H_0^1(\Omega_i)]^2}}.$$

496

497 We apply again the continuity of $a_i(\cdot, \cdot)$

$$498 \quad \left| \int_0^t a_i(\mathbf{e}_i^\ell(s), \mathbf{v}) ds \right| \leq M_i \int_0^t \|\mathbf{e}_i^\ell(s)\|_{X_i} \|\mathbf{v}\|_{X_i} ds \leq M_i \|\mathbf{v}\|_{[H_0^1(\Omega_i)]^2} \sqrt{T} \|\mathbf{e}_i^\ell\|_{L^2((0,T), X_i)}$$

499

500 as well as the Cauchy-Schwarz and Poincaré inequalities on $(\mathbf{e}_i^\ell(t), \mathbf{v})_{\Omega_i}$, we get

$$501 \quad \|D_i^\ell - \frac{1}{|\Omega_i|} \int_{\Omega_i} D_i^\ell\|_{\Omega_i} \leq \frac{1}{\gamma_3} \left[C_{P_i} \|\mathbf{e}_i^\ell(t)\|_{\Omega_i} + M_i \sqrt{T} \|\mathbf{e}_i^\ell\|_{L^2((0,T), X_i)} \right]$$

502

503 with C_{P_i} the Poincaré constant of Ω_i . From the convergence of the velocity, we get
504 the corollary. \square

505 *Remark 6.4.* Corollary 6.3 tells us that, when ℓ grows, the (time primitive of
506 the) pressure converges to 0, up to constant values in space, possibly depending on
507 the subdomain Ω_i and iteration count ℓ . And, indeed, numerical results given in
508 Section 10 show that pressure iterates do not converge to the monodomain solution,
509 unless a correction is applied, which is the object of the next Section.

510 **7. Recovering the pressure.** Let us introduce the notation $\langle p \rangle_{\mathcal{O}} = \frac{1}{|\mathcal{O}|} \int_{\mathcal{O}} p dx$ for
511 the mean value of a function on a domain \mathcal{O} (whatever the space dimension of \mathcal{O}).

512 We set $d_i^\ell := p_i - p_i^\ell$, $i \in \llbracket 1, M \rrbracket$, and recall that h_{ij}^ℓ is defined in (6.3).

513 *Hypothesis 7.1.* In this section, we suppose that, for a.e $t \in (0, T)$

- 514 • $\|d_i^\ell - \langle d_i^\ell \rangle_{\Omega_i}\|_{\Omega_i} \rightarrow 0$ for all i when $\ell \rightarrow +\infty$
- 515 • $\langle \langle d_i^\ell \rangle_{\Gamma_{ij}} - \langle d_i^\ell \rangle_{\Omega_i} \rangle$ tends to 0 for all $j \in \mathcal{I}_i$, for all i , when $\ell \rightarrow +\infty$
- 516 • $\langle \langle h_{ij}^\ell \rangle_{\Gamma_{ij}} + \alpha_{ij} \langle d_i^\ell \rangle_{\Gamma_{ij}} \rangle \rightarrow 0$ for all $j \in \mathcal{I}_i$, for all i , when $\ell \rightarrow +\infty$

517 *Remark 7.2.* The above hypothesis can be implied from stronger assumptions on
518 the regularity and convergence of the velocity. Indeed, suppose that $(\mathbf{e}_i^\ell, d_i^\ell)$ is the
519 strong solution of the following Robin problem

$$\begin{aligned} \partial_t \mathbf{e}_i^\ell - \nu \Delta \mathbf{e}_i^\ell + \nabla d_i^\ell &= 0 & \text{in } & \Omega_i \times (0, T) \\ \nabla \cdot \mathbf{e}_i^\ell &= 0 & \text{in } & \Omega_i \times (0, T) \\ \mathbf{e}_i^\ell(\cdot, t=0) &= 0 & \text{in } & \Omega_i \\ \mathbf{e}_i^\ell &= 0 & \text{on } & (\partial\Omega \cap \partial\Omega_i) \times (0, T) \\ \alpha_{ij} (\nu \partial_{\mathbf{n}_{ij}} \mathbf{e}_i^\ell \cdot \mathbf{n}_{ij} - d_i^\ell) + \mathbf{e}_i^\ell \cdot \mathbf{n}_{ij} &= h_{ij}^\ell & \text{on } & \Gamma_{ij} \times (0, T) \\ \beta_{ij} \nu \partial_{\mathbf{n}_{ij}} \mathbf{e}_i^\ell \times \mathbf{n} + \mathbf{e}_i^\ell \times \mathbf{n}_{ij} &= \zeta_{ij}^\ell & \text{on } & \Gamma_{ij} \times (0, T) \end{aligned}$$

520

521

522 with the following convergence

$$523 \quad \|\mathbf{e}_i^\ell\|_{L^\infty((0,T), [H^2(\Omega_i)]^2)} \rightarrow 0, \quad \|\partial_t \mathbf{e}_i^\ell\|_{L^\infty((0,T), [L^2(\Omega_i)]^2)} \rightarrow 0.$$

524

525 From this, we get, for a.e. $t \in (0, T)$, $\|\nabla d_i^\ell(t)\|_{\Omega_i} \rightarrow 0$, which implies the first and
526 second items in Hypothesis 7.1. This also implies the convergence of trace of the
527 velocity: for a.e. $t \in (0, T)$, we have $\|\alpha_{ij} \nu \partial_{\mathbf{n}_{ij}} \mathbf{e}_i^\ell(t) \cdot \mathbf{n}_{ij} + \mathbf{e}_i^\ell(t) \cdot \mathbf{n}_{ij}\|_{\Gamma_{ij}} \rightarrow 0$ that
528 leads to the third item in Hypothesis 7.1.

529 One can rewrite the three items in Hypothesis 7.1 on the error as follows :
530 when $\ell \rightarrow +\infty$, $\forall i \in \llbracket 1, M \rrbracket$,

$$531 \quad \|(p_i^\ell - p_i) - \langle \langle p_i^\ell \rangle_{\Omega_i} - \langle p_i \rangle_{\Omega_i} \rangle\|_{\Omega_i} \rightarrow 0, \quad (7.1)$$

$$532 \quad \langle \langle p_i^\ell - p_i \rangle_{\Gamma_{ij}} - \langle \langle p_i^\ell - p_i \rangle_{\Omega_i} \rangle \rangle \rightarrow 0, \quad \forall j \in \mathcal{I}_i, \quad (7.2)$$

$$533 \quad \langle \langle g_{ij}^\ell \rangle_{\Gamma_{ij}} - \langle g_{ij} \rangle_{\Gamma_{ij}} \rangle + \alpha_{ij} \langle \langle p_i^\ell - p_i \rangle_{\Gamma_{ij}} \rangle \rightarrow 0, \quad \forall j \in \mathcal{I}_i. \quad (7.3)$$

534

535 Expression (7.1) shows that $p_i^\ell(t)$ will tend to $p_i(t)$ if and only if the mean-value of $p_i^\ell(t)$
 536 on Ω_i tends to the mean value of $p_i(t)$. However, no constraint was imposed on the
 537 mean-value of $p_i^\ell(t)$ in the algorithm, since, thanks to the Robin boundary conditions,
 538 such constraint is not necessary to obtain local well-posed problems at each iteration.
 539 In Section 5, we observed cases in which p_i^ℓ does not converge to the monodomain
 540 solution p_i . In this section, we build a modified pressure \tilde{p}_i^ℓ such that $\tilde{p}_i^\ell(t)$ tends
 541 to $p_i(t)$ in $L^2(\Omega_i)$, $i = 1, \dots, M$.
 542 Let us denote $X_i(t) := \langle p_i(t) \rangle_{\Omega_i}$, $\forall i \in \llbracket 1, M \rrbracket$. Then, using this notation, (7.1) reads

$$543 \quad \|(p_i^\ell(t) - \langle p_i^\ell(t) \rangle_{\Omega_i} + X_i(t)) - p_i(t)\|_{L^2(\Omega_i)} \longrightarrow 0 \text{ when } \ell \rightarrow \infty. \quad (7.4)$$

545 From (7.4), we see that $(p_i^\ell(t) - \langle p_i^\ell(t) \rangle_{\Omega_i} + X_i(t))$ is the right approximation to
 546 calculate at each iteration since it tends to $p_i(t)$. However, we do not know how to
 547 calculate it because X_i is not known. A similar question was raised in the thesis of
 548 Lissoni [33, Theorem IV.3.9] at the discrete level, within a Schwarz algorithm applied
 549 at each time step of a time marching scheme for the numerical approximation of the
 550 incompressible Navier-Stokes equations.

551 We introduce below a new quantity $Y_i^\ell(t)$, fully computable at any given iteration ℓ ,
 552 that tends to $X_i(t)$ when ℓ tends to infinity, from which we will define the modified
 553 pressure \tilde{p}_i^ℓ .

554 To ease the presentation, we shall set $|\Gamma_{ij}| = 0$, $\alpha_{ij} = 0$ and $g_{ij}^\ell = 0$ if $j \notin \mathcal{I}_i$.
 555 Moreover, we introduce the constant matrix

$$556 \quad A = (a_{ij})_{1 \leq i, j \leq M}, \quad \text{with} \quad a_{ii} = \sum_{j=1, j \neq i}^M |\Gamma_{ij}| \alpha_{ij}, \text{ and } a_{ij} = -|\Gamma_{ji}| \alpha_{ji} \text{ if } j \neq i$$

558 together with the constant vector $C = (|\Omega_1|, |\Omega_2|, \dots, |\Omega_M|)$ and the sequence of
 559 vectors $(B^\ell)_\ell$, with $B^\ell = (B_1^\ell, B_2^\ell, \dots, B_M^\ell)^t$ defined as

$$560 \quad B_i^\ell = \sum_{j=1}^M |\Gamma_{ij}| [\langle g_{ij}^\ell \rangle_{\Gamma_{ij}} + \alpha_{ij} \langle p_i^\ell \rangle_{\Omega_i}] - \sum_{j=1}^M |\Gamma_{ji}| [\langle g_{ji}^\ell \rangle_{\Gamma_{ji}} + \alpha_{ji} \langle p_j^\ell \rangle_{\Omega_j}].$$

563 **THEOREM 7.3.** *Assume that $\alpha_{ij} = \alpha_{ji}$, $\forall (i, j)$. We have the following properties*

564 (i) *For all ℓ , the following system*

$$565 \quad \begin{aligned} AY^\ell &= B^\ell, \\ CY^\ell &= 0, \end{aligned} \quad (7.5)$$

567 *has a unique solution $Y^\ell \in \mathbb{R}^M$.*

568 (ii) *Moreover, we have $Y^\ell \rightarrow X := (X_1, X_2, \dots, X_M)$ in \mathbb{R}^M , and for all t*

$$569 \quad \|\tilde{p}_i^\ell - p_i\|_{L^2(\Omega_i)} \longrightarrow 0, \text{ when } \ell \rightarrow \infty, \text{ with } \tilde{p}_i^\ell(t) := p_i^\ell(t) - \langle p_i^\ell(t) \rangle_{\Omega_i} + Y_i^\ell(t). \quad (7.6)$$

570 *Proof of (i).* The proof of Theorem 7.3–(i) relies on two main steps:

- 571 (a) Existence of solutions to the system $AY^\ell = B^\ell$,
 572 (b) Existence and uniqueness of a solution to system (7.5) thanks to the additional
 573 constraint $CY^\ell = 0$.

574 Let us start with (a). Because $\alpha_{ij} = \alpha_{ji}$, it holds that A is symmetric and then
 575 existence of at least one solution to the system $AY^\ell = B^\ell$ is equivalent to proving
 576 that $B^\ell \in \text{Im}(A) = (\text{Ker}(A))^\perp$. Thus, we start with the determination of $\text{Ker}(A)$.

577 Let $Y = (Y_1, Y_2, \dots, Y_M)^t \in \text{Ker}(A)$. Then, we have $\sum_{j=1}^M a_{ij}Y_j = 0, \forall i \in \llbracket 1, M \rrbracket$.

578 As $\alpha_{ij} = \alpha_{ji}$, we have $a_{ii} = -\sum_{j=1, j \neq i}^M a_{ij}$, which implies

$$579 \quad 0 = \sum_{j=1}^M a_{ij}Y_jY_i = \left(\sum_{j=1, j \neq i}^M a_{ij}Y_jY_i \right) + a_{ii}Y_i^2 = \sum_{j=1, j \neq i}^M a_{ij}(Y_jY_i - Y_i^2).$$

581 Summing the above expression in i , and using that $a_{ij} = a_{ji}$, we obtain

$$582 \quad \sum_{i=1}^M \sum_{j=1, j \neq i}^M a_{ij}(Y_jY_i - Y_i^2) = \sum_{i < j} a_{ij}(Y_i - Y_j)^2 = 0.$$

584 As $a_{ij} \leq 0$ for all (i, j) with $i \neq j$, and $a_{ij} < 0$ as soon as subdomains i and j are
 585 neighbours, this implies that $Y_i = Y_j$ for any pair of neighbouring subdomains i and j .
 586 Since Ω is connected, this finally implies that all Y_i are equal i.e. $\text{Ker}(A) = \text{span}(\mathbf{e})$
 587 with $\mathbf{e} = (1, 1, \dots, 1, 1)$. Then, $B^\ell \in (\text{Ker}(A))^\perp$ is equivalent to $B^\ell \cdot \mathbf{e} = \sum_{i=1}^M B_i^\ell = 0$.
 588 This is proved in the following way:

$$589 \quad \sum_{i=1}^M B_i^\ell = \sum_{i=1}^M \left[\sum_{j=1}^M |\Gamma_{ij}| (\langle g_{ij}^\ell \rangle_{\Gamma_{ij}} + \alpha_{ij} \langle p_i^\ell \rangle_{\Omega_i}) - \sum_{j=1}^M |\Gamma_{ji}| (\langle g_{ji}^\ell \rangle_{\Gamma_{ji}} + \alpha_{ji} \langle p_j^\ell \rangle_{\Omega_j}) \right].$$

591 Denoting $\Delta_{ij} := |\Gamma_{ij}| (\langle g_{ij}^\ell \rangle_{\Gamma_{ij}} + \alpha_{ij} \langle p_i^\ell \rangle_{\Omega_i})$, we obtain

$$592 \quad \sum_{i=1}^M B_i^\ell = \sum_{i=1}^M \sum_{j=1}^M \Delta_{ij} - \sum_{i=1}^M \sum_{j=1}^M \Delta_{ji} = 0.$$

594 Let us now turn to (b). From (a), we know that there exists at least a solution
 595 to $AY = B$; we let Y^* be such a solution. All other solutions may be written as
 596 $Y = Y^* + \mu \mathbf{e}$, with $\mu \in \mathbb{R}$. Existence of a solution to (7.5) follows from the fact
 597 that $C\mathbf{e} = |\Omega| \neq 0$: Choosing $\mu = -\frac{1}{|\Omega|}CY^*$ leads to $CY = CY^* + \mu C\mathbf{e} = 0$
 598 and then Y solves (7.5). As far as uniqueness is concerned, let Y_1 and Y_2 be two
 599 solutions of (7.5); since $(Y_1 - Y_2) \in \text{Ker}(A)$, then $(Y_1 - Y_2) = \tau \mathbf{e}$, with $\tau \in \mathbb{R}$. Since
 600 $\tau|\Omega| = \tau C\mathbf{e} = C(Y_1 - Y_2) = 0$ it follows that $\tau = 0$ and $Y_1 = Y_2$. This ends the proof
 601 of Theorem 7.3-(i). \square

602 *Proof of Theorem 7.3-(ii).* It relies on the two main results:

603 (c) $B^\ell \rightarrow AX$ in \mathbb{R}^M ,

604 (d) $CX = 0$.

605 Let us prove (c): from the divergence-free property of \mathbf{u}_i , we have

$$606 \quad 0 = \int_{\Omega_i} \nabla \cdot \mathbf{u}_i = \int_{\partial\Omega_i} \mathbf{u}_i \cdot \mathbf{n}_{\partial\Omega_i} = \sum_{j \in \mathcal{I}_i} \int_{\Gamma_{ij}} \mathbf{u}_i \cdot \mathbf{n}_{ij}. \quad (7.7)$$

607 Moreover, from the definition of g_{ij} in (6.1a) and the physical transmission condi-
 608 tions (2.4), we have

$$609 \quad |\Gamma_{ij}| \langle g_{ij} \rangle_{\Gamma_{ij}} - |\Gamma_{ji}| \langle g_{ji} \rangle_{\Gamma_{ji}} = \int_{\Gamma_{ij}} (g_{ij} - g_{ji}) = 2 \int_{\Gamma_{ij}} \mathbf{u}_i \cdot \mathbf{n}_{ij}. \quad (7.8)$$

610 Hence, from (7.7) and (7.8) we get

$$611 \quad \sum_{j \in \mathcal{I}_i} |\Gamma_{ij}| \langle g_{ij} \rangle_{\Gamma_{ij}} = \sum_{j \in \mathcal{I}_i} |\Gamma_{ji}| \langle g_{ji} \rangle_{\Gamma_{ji}}. \quad (7.9)$$

613 Expression (7.3) is equivalent to

$$614 \quad \langle g_{ij}^\ell \rangle_{\Gamma_{ij}} + \alpha_{ij} \langle p_i^\ell - p_i \rangle_{\Gamma_{ij}} \longrightarrow \langle g_{ij} \rangle_{\Gamma_{ij}}. \quad (7.10)$$

615 From (7.2), we may replace $\langle p_i^\ell - p_i \rangle_{\Gamma_{ij}}$ by $\langle p_i^\ell - p_i \rangle_{\Omega_i}$ in (7.10), then multiply by $|\Gamma_{ij}|$
616 and sum over $j \in \mathcal{I}_i$ for a given i to obtain

$$617 \quad \sum_{j \in \mathcal{I}_i} |\Gamma_{ij}| [\langle g_{ij}^\ell \rangle_{\Gamma_{ij}} + \alpha_{ij} \langle p_i^\ell - p_i \rangle_{\Omega_i}] \longrightarrow \sum_{j \in \mathcal{I}_i} |\Gamma_{ij}| \langle g_{ij} \rangle_{\Gamma_{ij}}. \quad (7.11)$$

619 In exactly the same way, we also obtain

$$620 \quad \sum_{j \in \mathcal{I}_i} |\Gamma_{ji}| [\langle g_{ji}^\ell \rangle_{\Gamma_{ji}} + \alpha_{ji} \langle p_j^\ell - p_j \rangle_{\Omega_j}] \longrightarrow \sum_{j \in \mathcal{I}_i} |\Gamma_{ji}| \langle g_{ji} \rangle_{\Gamma_{ji}}. \quad (7.12)$$

622 Using (7.11), (7.12) and (7.9), we obtain

$$623 \quad \sum_{j \in \mathcal{I}_i} |\Gamma_{ij}| [\langle g_{ij}^\ell \rangle_{\Gamma_{ij}} + \alpha_{ij} \langle p_i^\ell \rangle_{\Omega_i} - \alpha_{ij} \langle p_i \rangle_{\Omega_i}] \\ 624 \quad - \sum_{j \in \mathcal{I}_i} |\Gamma_{ji}| [\langle g_{ji}^\ell \rangle_{\Gamma_{ji}} + \alpha_{ji} \langle p_j^\ell \rangle_{\Omega_j} - \alpha_{ji} \langle p_j \rangle_{\Omega_j}] \longrightarrow 0,$$

626 or equivalently

$$627 \quad \sum_{j \in \mathcal{I}_i} |\Gamma_{ij}| [\langle g_{ij}^\ell \rangle_{\Gamma_{ij}} + \alpha_{ij} \langle p_i^\ell \rangle_{\Omega_i}] - \sum_{j \in \mathcal{I}_i} |\Gamma_{ji}| [\langle g_{ji}^\ell \rangle_{\Gamma_{ji}} + \alpha_{ji} \langle p_j^\ell \rangle_{\Omega_j}] \\ 628 \quad \longrightarrow \sum_{j \in \mathcal{I}_i} |\Gamma_{ij}| \alpha_{ij} \langle p_i \rangle_{\Omega_i} - \sum_{j \in \mathcal{I}_i} |\Gamma_{ji}| \alpha_{ji} \langle p_j \rangle_{\Omega_j}.$$

630 This is exactly $B^\ell \longrightarrow AX$.

631 Let us now prove (d): We have

$$632 \quad \int_{\Omega} p_i = \sum_{i=1}^M \int_{\Omega_i} p_i = \sum_{i=1}^M |\Omega_i| \langle p_i \rangle_{\Omega_i} = 0,$$

634 i.e. $CX = 0$.

635 We now prove Theorem 7.3–(ii): From the solution Y^ℓ of (7.5) given by Theo-
637 rem 7.3–(i), and from (c) and (d), we have $A(Y^\ell - X) \longrightarrow 0$ and $C(Y^\ell - X) = 0$.
638 Uniqueness of a solution to $AZ = B$ and $CZ = 0$ as soon as B is in $\text{Im}(A)$ and finite
639 dimension now imply that $(Y^\ell - X) \longrightarrow 0$ when $\ell \rightarrow \infty$. Then, from (7.4), with a
640 triangle inequality, we get (7.6). \square

641 *Remark 7.4.* In the general case of M subdomains, the calculation of \tilde{p}_i^ℓ is done
642 only once, at the last OSWR iteration. It involves solving the coarse problem (7.5)
643 when $M > 2$, and is given by an explicit formula when $M = 2$ (see Corollary 7.6),
644 thus the cost of calculating the modified pressure is negligible.

Remark 7.5. Recovering the correct pressure could also be performed from the fact that $\nabla(p_i^\ell - p_i)$ tends to zero when $\ell \rightarrow \infty$. Indeed, for a given Ω_i , choosing first an arbitrary point $\mathbf{x}_i \in \Omega_i$, then one may write

$$p_i(\mathbf{x}) = p_i(\mathbf{x}_i) + (\mathbf{x} - \mathbf{x}_i) \cdot \int_0^1 \nabla p_i(\mathbf{x}_i + t(\mathbf{x} - \mathbf{x}_i)) dt, \quad \forall \mathbf{x} \in \Omega_i.$$

645 Then, one could replace ∇p_i by ∇p_i^ℓ to obtain approximate values of the pressure at
 646 each point \mathbf{x} . However, this formula holds on a given subdomain Ω_i . In order to relate
 647 values of the pressures in Ω_i to those in a neighboring subdomain Ω_j through this
 648 kind of formula, one needs to choose a point on the boundary Γ_{ij} that will serve as
 649 the point \mathbf{x}_j in the subdomain Ω_j , and so on. At the discrete level, there are several
 650 drawbacks to that: this requires further communications between subdomains, the
 651 pressure gradient at the boundaries may not be easy to define (e.g. when the pressure
 652 is defined as a piecewise constant field like in the Crouzeix-Raviart finite element),
 653 and finally there are many ways to go from one cell to another in the mesh, and, due
 654 to round-off errors, this may lead to different evaluations of the pressure at a given
 655 cell in particular in very large scale computations.

656 In the two-subdomain case, we use the same notation as in Section 5. Then the
 657 calculation of \tilde{p}_i^ℓ can be done by the following explicit formula.

658 **COROLLARY 7.6.** *Let $M = 2$, $\alpha = \alpha_1 = \alpha_2$, and define, for $i = 1, 2$ and $j = 3 - i$,*

$$659 \quad \tilde{p}_i^\ell = p_i^\ell + \frac{|\Omega_j|}{|\Omega|} \left[\frac{1}{\alpha} (\langle g_i^\ell \rangle_\Gamma - \langle g_j^\ell \rangle_\Gamma) \right] - \frac{|\Omega_i|}{|\Omega|} \langle p_i^\ell \rangle_{\Omega_i} - \frac{|\Omega_j|}{|\Omega|} \langle p_j^\ell \rangle_{\Omega_j}.$$

660 *Then \tilde{p}_i^ℓ tends to p_i when ℓ tends to infinity, for $i = 1, 2$.*

661 *Proof.* For $M = 2$ we have

$$662 \quad B_1^\ell = -B_2^\ell = |\Gamma| [\langle g_1^\ell \rangle_\Gamma + \alpha \langle p_1 \rangle_{\Omega_1}] - |\Gamma| [\langle g_2^\ell \rangle_\Gamma + \alpha \langle p_2 \rangle_{\Omega_2}],$$

$$663 \quad \mathbf{A} = \begin{bmatrix} \alpha |\Gamma| & -\alpha |\Gamma| \\ -\alpha |\Gamma| & \alpha |\Gamma| \end{bmatrix},$$

$$664 \quad C = [|\Omega_1| \quad |\Omega_2|].$$

666 System (7.5) for $M = 2$ has a unique solution given by

$$667 \quad Y_1^\ell = \frac{|\Omega_2|}{|\Omega|} \left[\frac{1}{\alpha} (\langle g_1^\ell \rangle_\Gamma - \langle g_2^\ell \rangle_\Gamma) + (\langle p_1^\ell \rangle_{\Omega_1} - \langle p_2^\ell \rangle_{\Omega_2}) \right],$$

$$668 \quad Y_2^\ell = \frac{|\Omega_1|}{|\Omega|} \left[\frac{1}{\alpha} (\langle g_2^\ell \rangle_\Gamma - \langle g_1^\ell \rangle_\Gamma) + (\langle p_2^\ell \rangle_{\Omega_2} - \langle p_1^\ell \rangle_{\Omega_1}) \right].$$

670 From theorem 7.3, we have

$$671 \quad p_1^\ell - \langle p_1^\ell \rangle_{\Omega_1} + Y_1^\ell = p_1^\ell + \frac{|\Omega_2|}{|\Omega|} \left[\frac{1}{\alpha} (\langle g_1^\ell \rangle_\Gamma - \langle g_2^\ell \rangle_\Gamma) \right] - \frac{|\Omega_1|}{|\Omega|} \langle p_1^\ell \rangle_{\Omega_1} - \frac{|\Omega_2|}{|\Omega|} \langle p_2^\ell \rangle_{\Omega_2} \rightarrow p_1$$

$$672 \quad p_2^\ell - \langle p_2^\ell \rangle_{\Omega_2} + Y_2^\ell = p_2^\ell + \frac{|\Omega_1|}{|\Omega|} \left[\frac{1}{\alpha} (\langle g_2^\ell \rangle_\Gamma - \langle g_1^\ell \rangle_\Gamma) \right] - \frac{|\Omega_1|}{|\Omega|} \langle p_1^\ell \rangle_{\Omega_1} - \frac{|\Omega_2|}{|\Omega|} \langle p_2^\ell \rangle_{\Omega_2} \rightarrow p_2 \square$$

674 **8. Convergence factor via Fourier transform.** The aim of this section is to find a
 675 way to conveniently choose the parameters (α, β) that play an important role in the
 676 actual rate of convergence in numerical experiments.

677 Let $\Omega = \mathbb{R}^2$. We consider two subdomains $\Omega_1 = (-\infty, 0) \times \mathbb{R}$ and $\Omega_2 = (0, +\infty) \times \mathbb{R}$,
 678 as commonly done for the analysis of OSWR methods. To simplify notation, we set
 679 $\Gamma := \Gamma_{12} = \Gamma_{21} = \{x = 0\} \times \mathbb{R}$, and denote α_{12} and α_{21} by α_1 and α_2 , respectively.
 680 We denote $\mathbf{u} = (u, v)$ the two components of the velocity and set $\mathbf{f} = (f_x, f_y)$. Recall
 681 here the Stokes problem

$$\begin{aligned} \partial_t u - \nu \Delta u + \partial_x p &= f_x \\ \partial_t v - \nu \Delta v + \partial_y p &= f_y \quad , \text{ in } \quad \Omega \times (0, T) \\ \partial_x u + \partial_y v &= 0 \\ u(\cdot, t=0) &= u_0 \\ v(\cdot, t=0) &= v_0 \quad , \text{ in } \quad \Omega \\ u, v &\rightarrow 0 \quad , \text{ when } \quad |(x, y)| \rightarrow +\infty. \end{aligned}$$

684 We write the algorithm for the errors using the same notation (u, v, p) , which means
 685 that, by linearity, we set $f_x = f_y = 0$ and $u_0 = v_0 = 0$. To avoid additional notation
 686 for the Robin terms, we write the OSWR algorithm as follows: starting with u_i^0, v_i^0, p_i^0 ,
 687 at step $\ell \geq 1$ and provided $u_i^{\ell-1}, v_i^{\ell-1}, p_i^{\ell-1}$ we solve

$$\begin{aligned} \partial_t u_i^\ell - \nu \Delta u_i^\ell + \partial_x p_i^\ell &= 0 \\ \partial_t v_i^\ell - \nu \Delta v_i^\ell + \partial_y p_i^\ell &= 0 \quad , \text{ in } \quad \Omega_i \times (0, T) \\ \partial_x u_i^\ell + \partial_y v_i^\ell &= 0 \\ u_i^\ell(\cdot, t=0) &= 0 \\ v_i^\ell(\cdot, t=0) &= 0 \quad , \text{ in } \quad \Omega_i \\ u_i^\ell, v_i^\ell &\rightarrow 0 \quad \text{ when } \quad |(x, y)| \rightarrow +\infty \end{aligned}$$

690 together with transmission condition on $\Gamma \times (0, T)$, for $i = 1, 2$ and $j = 3 - i$:

$$\begin{aligned} \alpha_i(\nu \partial_x u_i^\ell - p_i^\ell) + (-1)^{i+1} u_i^\ell &= \alpha_i(\nu \partial_x u_j^{\ell-1} - p_j^{\ell-1}) + (-1)^{i+1} u_j^{\ell-1} \\ \nu \beta_i \partial_x v_i^\ell + (-1)^{i+1} v_i^\ell &= \nu \beta_i \partial_x v_j^{\ell-1} + (-1)^{i+1} v_j^{\ell-1} \end{aligned}$$

694 Let us consider the system in Ω_1 , and let $\ell \geq 1$. Taking the Fourier transform in time
 695 and in y -direction with time frequency ω and space frequency $k \neq 0$, and, for the sake
 696 of simplicity, keeping notation u, v instead of \hat{u}, \hat{v} , we get

$$i\omega u_1^\ell - \nu \partial_{xx} u_1^\ell + \nu k^2 u_1^\ell + \partial_x p_1^\ell = 0, \quad (8.1a)$$

$$i\omega v_1^\ell - \nu \partial_{xx} v_1^\ell + \nu k^2 v_1^\ell + ik p_1^\ell = 0, \quad (8.1b)$$

$$\partial_x u_1^\ell + ik v_1^\ell = 0. \quad (8.1c)$$

701 By differentiating equation (8.1b) with respect to x , multiplying (8.1a) by $(-ik)$, and
 702 summing the resulting equations, and denoting $w_1^\ell := \partial_x v_1^\ell - ik u_1^\ell$ the vorticity, we
 703 get the vorticity equation

$$i\omega w_1^\ell - \nu \partial_{xx} w_1^\ell + \nu k^2 w_1^\ell = 0. \quad (8.2)$$

706 Denote by $\lambda = \sqrt{k^2 + \frac{i\omega}{\nu}}$ with positive real part. As w_1 vanishes at $-\infty$, one gets

$$w_1^\ell = E^\ell \exp(\lambda x) \quad (8.3)$$

709 Using the definition of w_1 and differentiating (8.1c), we get, for u_1

$$710 \quad \partial_{xx} u_1^\ell - k^2 u_1^\ell = -ikw_1^\ell. \quad (8.4)$$

712 The homogeneous equation associated to (8.4) has characteristic roots $\pm|k|$. As u_1
713 and v_1 vanish at $-\infty$, we only retain the root $|k|$. Given the form (8.3) of the right-
714 hand side of (8.4), its solution can be written under the form

$$715 \quad u_1^\ell = A^\ell \exp(|k|x) + B^\ell \exp(\lambda x),$$

717 with $A^\ell, B^\ell \in \mathbb{C}$. Then, using (8.1c) and (8.1b), we get

$$718 \quad v_1^\ell = A^\ell \frac{i|k|}{k} \exp(|k|x) + B^\ell \frac{i\lambda}{k} \exp(\lambda x),$$

$$719 \quad p_1^\ell = -A^\ell \frac{i\omega}{|k|} \exp(|k|x). \quad 720$$

721 Similarly, for domain Ω_2 , there exist $C^\ell, D^\ell \in \mathbb{C}$ such that

$$722 \quad u_2^\ell = C^\ell \exp(-|k|x) + D^\ell \exp(-\lambda x)$$

$$723 \quad v_2^\ell = -C^\ell \frac{i|k|}{k} \exp(-|k|x) - D^\ell \frac{i\lambda}{k} \exp(-\lambda x)$$

$$724 \quad p_2^\ell = C^\ell \frac{i\omega}{|k|} \exp(-|k|x) \quad 725$$

726 Replacing the above expressions in the transmission conditions, we obtain

$$727 \quad \alpha_1(\nu|k|A^\ell + \nu\lambda B^\ell + \frac{i\omega}{|k|}A^\ell) + A^\ell + B^\ell =$$

$$728 \quad \alpha_1(-\nu|k|C^{\ell-1} - \nu\lambda D^{\ell-1} - \frac{i\omega}{|k|}C^{\ell-1}) + C^{\ell-1} + D^{\ell-1},$$

$$729 \quad \nu\beta_1(ikA^\ell + \frac{i\lambda^2}{k}B^\ell) + \frac{i|k|}{k}A^\ell + \frac{i\lambda}{k}B^\ell =$$

$$730 \quad \nu\beta_1(ikC^{\ell-1} + \frac{i\lambda^2}{k}D^{\ell-1}) - \frac{i|k|}{k}C^{\ell-1} - \frac{i\lambda}{k}D^{\ell-1} \quad 731$$

732 and

$$733 \quad \alpha_2(-\nu|k|C^\ell - \nu\lambda D^\ell - \frac{i\omega}{|k|}C^\ell) - C^\ell - D^\ell =$$

$$734 \quad \alpha_2(\nu|k|A^{\ell-1} + \nu\lambda B^{\ell-1} + \frac{i\omega}{|k|}A^{\ell-1}) - A^{\ell-1} - B^{\ell-1},$$

$$735 \quad \nu\beta_2(ikC^\ell + \frac{i\lambda^2}{k}D^\ell) + \frac{i|k|}{k}C^\ell + \frac{i\lambda}{k}D^\ell =$$

$$736 \quad \nu\beta_2(ikA^{\ell-1} + \frac{i\lambda^2}{k}B^{\ell-1}) - \frac{i|k|}{k}A^{\ell-1} - \frac{i\lambda}{k}B^{\ell-1}. \quad 737$$

738 These transmission conditions can be written in matrix form as follows :

$$739 \quad \mathcal{M}(\alpha_1, \beta_1) \begin{pmatrix} A^\ell \\ B^\ell \end{pmatrix} = \mathcal{N}(\alpha_1, \beta_1) \begin{pmatrix} C^{\ell-1} \\ D^{\ell-1} \end{pmatrix} \quad \text{and} \quad \mathcal{M}(\alpha_2, \beta_2) \begin{pmatrix} C^\ell \\ D^\ell \end{pmatrix} = \mathcal{N}(\alpha_2, \beta_2) \begin{pmatrix} A^{\ell-1} \\ B^{\ell-1} \end{pmatrix}$$

740 where

$$\mathcal{M}(\alpha, \beta) := \begin{bmatrix} 1 + \frac{\nu\alpha\lambda^2}{|k|} & 1 + \alpha\nu\lambda \\ \nu\beta k + \frac{|k|}{k} & \frac{\nu\beta\lambda^2}{k} + \frac{\lambda}{k} \end{bmatrix}, \quad \mathcal{N}(\alpha, \beta) := \begin{bmatrix} 1 - \frac{\nu\alpha\lambda^2}{|k|} & 1 - \alpha\nu\lambda \\ \nu\beta k - \frac{|k|}{k} & \frac{\nu\beta\lambda^2}{k} - \frac{\lambda}{k} \end{bmatrix}. \quad (8.5)$$

741

742 This leads to the following recurrent formulation

$$\begin{pmatrix} A^\ell \\ B^\ell \end{pmatrix} = \mathcal{R}(\alpha_1, \alpha_2, \beta_1, \beta_2) \begin{pmatrix} A^{\ell-2} \\ B^{\ell-2} \end{pmatrix}, \quad \forall \ell \geq 2, \quad (8.6)$$

744 where

$$\mathcal{R}(\alpha_1, \alpha_2, \beta_1, \beta_2) = \mathcal{M}^{-1}(\alpha_1, \beta_1)\mathcal{N}(\alpha_1, \beta_1)\mathcal{M}^{-1}(\alpha_2, \beta_2)\mathcal{N}(\alpha_2, \beta_2). \quad (8.7)$$

746 In view of (8.6), the convergence properties of the OSWR algorithm, and in particular
747 its rate, will depend on the spectral radius of the matrix \mathcal{R} defined in (8.7).

748 *Remark 8.1.* If one sets $\tilde{\alpha} := \nu\alpha$ and $\tilde{\beta} := \nu\beta$, as well as $\tilde{\omega} := \frac{\omega}{\nu}$, then matrices \mathcal{M}
749 and \mathcal{N} (defined in (8.5)), depend only on $\tilde{\alpha}$, $\tilde{\beta}$, on $\tilde{\omega}$ and on k . Thus, when ν varies,
750 the convergence rate remains unchanged if $\tilde{\alpha}$ and $\tilde{\beta}$ are kept constant and if the range
751 in which $\tilde{\omega}$ is considered does not change. As will be seen in Section 9, this is the
752 case if $\nu\Delta t$ and νT are kept unchanged. This observation coincides with the fact
753 that the non-dimensional form of the Stokes equation is not modified when νT is kept
754 constant.

755 *Remark 8.2.* When k tends to 0, the spectral radius of the matrix \mathcal{R} tends to 1.
756 This is coherent with what was observed in Section 5 and in Remarks 4.3 and 6.4,
757 which led us to the pressure correction described in Section 7.

758 *Remark 8.3.* When k and ω tend to $+\infty$, the spectral radius of the matrix \mathcal{R}
759 tends to 1. This implies that analysing the iteration matrix does not help to prove
760 the general convergence (for all frequencies) of the algorithm, and one always needs
761 the energy estimate technique of Section 6 (for another example, see [10]).

762 *Remark 8.4.* In practical experiments, all equations are discretized in space and
763 time. As far as space discretization is concerned, the solution of the discrete version
764 of (8.2) remains close to (8.3) if the space discretization parameter is small enough
765 with respect to $\sqrt{\frac{\nu}{\omega}}$; since ω is in practice bounded by $\frac{\pi}{\Delta t}$, we expect that the above
766 Fourier analysis may remain close to practical experiments if the term $\sqrt{\nu\Delta t}$ is large
767 enough compared to the space discretization parameter. This has indeed recently
768 been observed for the heat equation in [2]. As far as time discretization is concerned,
769 the inclusion of its effect in the convergence analysis of OSWR methods is a current
770 topic of research, and is for example addressed in [15] where a Z -transform is used
771 and in [2], where a discrete-time analysis of the OSWR method is proposed. This
772 issue is also addressed in Section 9.2.

773 **9. Optimized Robin parameters.** One can choose $\alpha_1, \alpha_2, \beta_1, \beta_2$ to minimize the
774 convergence factor of the continuous OSWR algorithm, defined in the above section.
775 Such parameters are called *continuous optimized parameters*. However, for the in-
776 compressible Stokes problem, we will see in the numerical experiments of Section 10
777 that better results can be obtained by minimizing the discrete-time counterpart of
778 this convergence factor. The corresponding parameters are then called *discrete-time*
779 *optimized parameters*. Both of these optimization procedures are described below.

9.1. Continuous optimized parameters. From Section 8, the convergence factor is $\varrho(\mathcal{R}(\alpha_1, \alpha_2, \beta_1, \beta_2, k, \omega))$, where \mathcal{R} is defined in (8.7), and $\varrho(\mathcal{R})$ denotes the spectral radius of \mathcal{R} . While we have $\max_{(k, \omega) \in \mathbb{R}^2} \varrho(\mathcal{R}(\alpha_1, \alpha_2, \beta_1, \beta_2, k, \omega)) = 1$, we can use this convergence factor to calculate Robin parameters for numerical computations, for which the frequencies k and ω are bounded (by frequencies relevant to the global space-time domain and the ones supported by the numerical grid). Thus, we set

$$\tilde{\rho}_c(\alpha_1, \alpha_2, \beta_1, \beta_2) := \max_{\frac{\pi}{L} \leq k \leq \frac{\pi}{h_\Gamma}, \frac{\pi}{T} \leq \omega \leq \frac{\pi}{\Delta t}} \varrho(\mathcal{R}(\alpha_1, \alpha_2, \beta_1, \beta_2, k, \omega)),$$

780 where L is a characteristic size of the computational domain and h_Γ is a measure of
781 the mesh step size on the interface (typically the mean-value of the segment lengths).

782 Let us consider the one-sided Robin case $\alpha := \alpha_1 = \alpha_2 = \beta_1 = \beta_2$, and set
783 $\rho_c(\alpha) := \tilde{\rho}_c(\alpha, \alpha, \alpha, \alpha)$. Then, the *continuous optimized Robin parameter* α_c is defined
784 as a solution of the following minimization problem :

$$785 \quad \rho_c(\alpha_c) = \min_{\alpha > 0} \rho_c(\alpha).$$

786 **9.2. Discrete-time optimized parameters.** One can also consider the semi-discrete
787 in time counterpart of the continuous convergence factor to better capture the discrete-
788 time frequencies, i.e. replace in the expression of \mathcal{R} the term $i\omega$ by its discrete counter-
789 part using the implicit Euler scheme, that is we replace $i\omega$ by $\frac{1-e^{-i\omega\Delta t}}{\Delta t}$. Equivalently,
790 we replace in the expression of \mathcal{R} (in (8.7)) the term ω by $\bar{\omega} := -i \left(\frac{1-e^{-i\omega\Delta t}}{\Delta t} \right)$, and
791 set $\mathcal{R}_{\Delta t}(\alpha_1, \alpha_2, \beta_1, \beta_2, k, \omega) := \mathcal{R}(\alpha_1, \alpha_2, \beta_1, \beta_2, k, \bar{\omega})$.

Then, as above, we define

$$\tilde{\rho}(\alpha_1, \alpha_2, \beta_1, \beta_2) := \max_{\frac{\pi}{L} \leq k \leq \frac{\pi}{h}, \frac{\pi}{T} \leq \omega \leq \frac{\pi}{\Delta t}} \varrho(\mathcal{R}_{\Delta t}(\alpha_1, \alpha_2, \beta_1, \beta_2, k, \omega)).$$

792 Let us consider the one-sided Robin case $\alpha := \alpha_1 = \alpha_2 = \beta_1 = \beta_2$, and define
793 $\rho(\alpha) := \tilde{\rho}(\alpha, \alpha, \alpha, \alpha)$. Then, the *Discrete-time (DT) optimized Robin parameter* α^* is
794 defined as a solution of the following minimization problem :

$$795 \quad \rho(\alpha^*) = \min_{\alpha > 0} \rho(\alpha).$$

796 *Remark 9.1.* One could also consider optimized Robin-2p parameters (α, β) with
797 $\alpha := \alpha_1 = \alpha_2$, $\beta := \beta_1 = \beta_2$, or 2-sided parameters (γ, δ) with $\gamma := \alpha_1 = \beta_1$,
798 $\delta := \alpha_2 = \beta_2$, that optimize the continuous or discrete-time convergence factors as
799 done in [9]. Given their additional complexity, these more general cases will not be
800 considered here, and are the subject of a subsequent article.

801 **10. Numerical results.** In this section, we present numerical experiments that il-
802 lustrate the performances of the OSWR method of Section 4, with Freefem++ [27].
803 For the space discretization we use the nonconforming Crouzeix-Raviart Finite Ele-
804 ment method in 2D (i.e. piecewise linear elements continuous only at the midpoints
805 of the edges of the mesh for the velocity $\mathbf{u} = (u_x, u_y)$, and piecewise constant \mathbb{P}_0
806 elements for the pressure p), and consider the backward Euler method for the time
807 discretization.

808 In what follows, the term "monodomain solution" will refer to the fully discrete
809 solution obtained on the global mesh without domain decomposition.

810 We set $\Omega =]0, 1[\times]0, 1[$, $T = 1$, and consider the Stokes problem (2.1), where the
811 value of the diffusion coefficient ν will be specified in each of the examples below.

812 From Remark 9.1, only one-sided Robin parameter $\alpha := \alpha_1 = \alpha_2 = \beta_1 = \beta_2$ will
 813 be considered. In particular, we will use the theoretical optimized values α_c and α^*
 814 defined in Section 9, which are calculated using the function `fminsearch` of MAT-
 815 LAB [37]. Random initial Robin data on the space-time interfaces will be used, unless
 816 specified.

817 In Section 10.1 some results are shown on the convergence of the OSWR algorithm,
 818 without and with modification of the pressure as in Section 7. In Section 10.2 we
 819 illustrate the influence of the Robin parameter on the convergence of the algorithm,
 820 and then in Section 10.3 we present results on a more realistic test case.

821 **10.1. Recovering the pressure: a rotating velocity example.** The diffusion coef-
 822 ficient is $\nu = 1$ and we choose the right-hand side \mathbf{f} and the values of the boundary
 823 and initial conditions so that the exact solution is given by

$$\begin{aligned} 824 \quad \mathbf{u}(\mathbf{x}, t) &= (-\cos(\pi y) \sin(\pi x) \cos(2\pi t), \sin(\pi y) \cos(\pi x) \cos(2\pi t)), \\ 825 \quad p(\mathbf{x}, t) &= \cos(t)(x^2 - y^2), \quad \forall \mathbf{x} \in \Omega, \forall t \in (0, T). \end{aligned}$$

827 On Figure 1 we show the velocity field \mathbf{u} (on the left), and the pressure p (on the
 right) at final time $t = 1$.

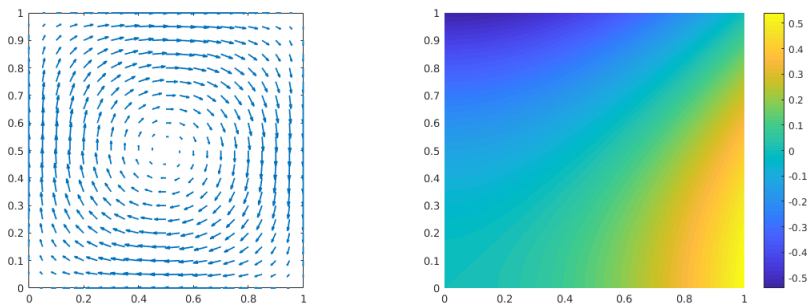


FIG. 1. *Example 1: rotating velocity field (left), and pressure (right)*

828 The domain Ω is decomposed into nine subdomains as in Figure 2, and two meshes
 829 will be considered (as shown on Figure 2), with mesh sizes $h = 0.0625$ and $h = 0.0312$
 830 respectively. To each mesh, the associated time step is $\Delta t = h$.

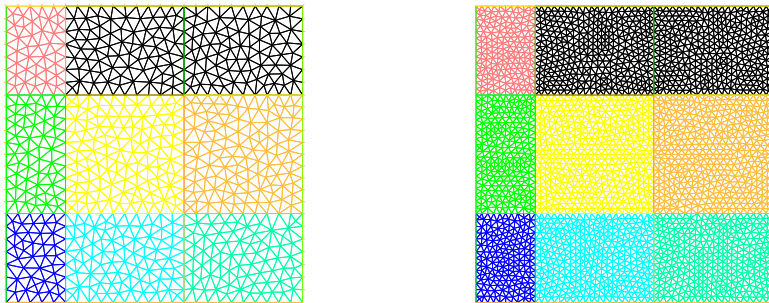


FIG. 2. *Example 1: mesh 1 (left) and mesh 2 (right)*

831

832 We choose $\alpha_1 = \alpha_2 = \beta_1 = \beta_2 = \alpha^*$, where α^* is the DT-Optimized Robin
 833 parameter defined in Section 9.1, whose value here is $\alpha^* \approx 3.0832 \times 10^{-1}$ for mesh 1
 834 and $\alpha^* \approx 2.2719 \times 10^{-1}$ for mesh 2.

835 On Figure 3 we show the evolution of the relative errors, of p , u_x and u_y , in the
 836 $L^\infty(0, T; L^2(\Omega))$ -norm, between the OSWR and monodomain solutions, as functions
 837 of the number OSWR iterations, for mesh 1 (left) and mesh 2 (right). The top
 838 figures are with non-modified pressure, and the bottom figures are with the modified
 839 pressure \tilde{p}_i^ℓ , $i = 1, 2$, at each iteration ℓ (defined in Section 7). We observe that,
 840 with the non-modified pressure, the method converges for the velocity but not for the
 841 pressure, as expected from the observations of Section 5 and Theorem 6.2. On the
 842 other hand, with the modified pressure, we see that the method now converges both
 for the velocity and the pressure, accordingly to Theorem 7.3.

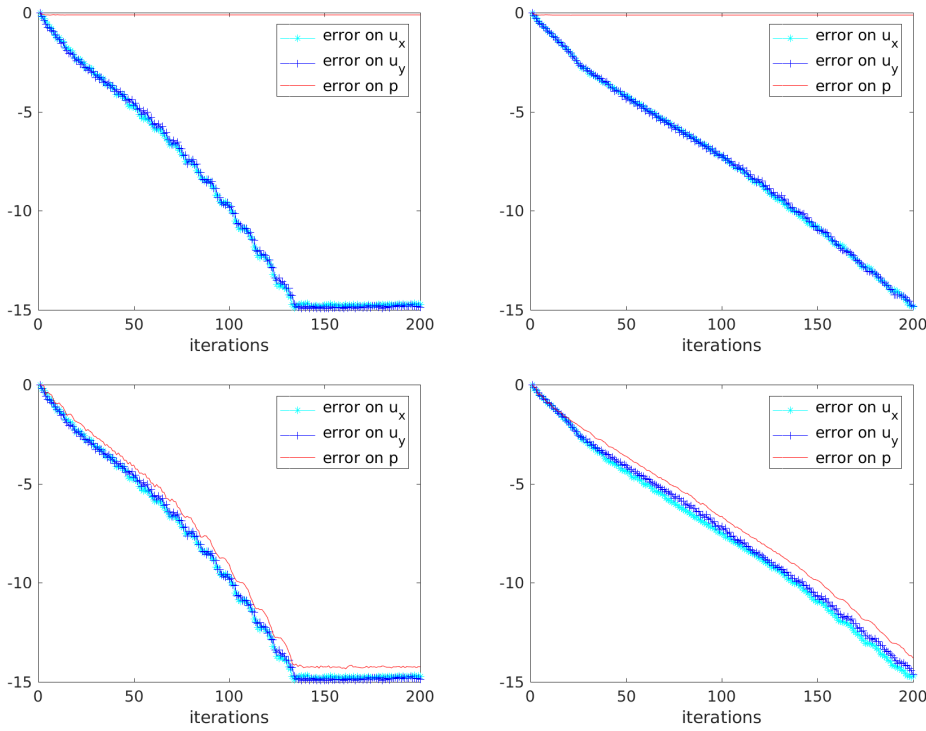


FIG. 3. Example 1: relative errors (for u_x , u_y and p) versus iterations with non-modified pressure (top), and modified pressure (bottom), for mesh 1 (left) and mesh 2 (right)

843

844 *Remark 10.1.* Even if we calculate a modified pressure at each iteration, we do
 845 not use it in the transmission conditions of Algorithm 4.1, thus this does not change
 846 the velocity convergence, as shown on Figure 3.

847 *Remark 10.2.* Here and in what follows, the pressure is modified at each iteration
 848 to illustrate the convergence of the multidomain solution to the monodomain one. A
 849 consequence of Remark 7.4 is that in practice one needs only to modify the pressure
 850 at the last OSWR iteration, which makes the cost of the modification negligible.

851 **10.2. Optimized Robin parameters.** The domain Ω is decomposed into two sub-
 852 domains as in Figure 4, and we consider the three uniform meshes of Figure 4, with

853 mesh sizes on the interface and associated time steps equal to $h_\Gamma = \Delta t = 1/12$,
 854 $h_\Gamma = \Delta t = 1/24$, and $h_\Gamma = \Delta t = 1/48$, respectively. In order to analyze the con-
 855 vergence behavior of the method, we simulate the error equations (i.e. we take ho-
 856 mogeneous initial and boundary conditions, and $\mathbf{f} = 0$). Thus, the OSWR solution
 857 converges to zero.

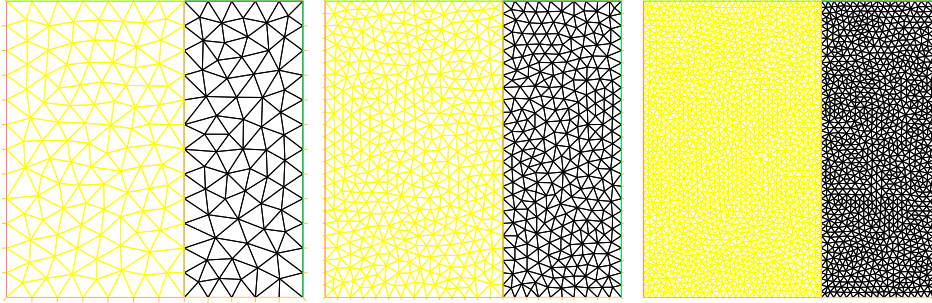


FIG. 4. Example 2: mesh 1 (left), mesh 2 (middle), and mesh 3 (right)

858 **10.2.1. Case with a fixed mesh and different values of ν .** We consider mesh 2 (i.e.
 859 $h_\Gamma = \Delta t = 1/24$). In Figure 5, we plot the evolution of the continuous convergence
 860 factor ρ_c (on the left) and of the discrete-time convergence factor ρ (on the right),
 861 as functions of the Robin parameter α , for different values of ν : $\nu = 1$ (solid line),
 862 $\nu = 0.5$ (dashed line), $\nu = 0.1$ (dash-dotted line), $\nu = 0.05$ (dotted line). The
 863 theoretical optimized values α_c (blue circle) and α^* (red star), are also shown. We
 864 observe that both α_c and α^* increase when ν decreases. However, the values of α_c
 865 and α^* are very different, and when ν decreases, α^* increases faster than α_c , with an
 associated $\rho(\alpha^*)$ that increases slower than $\rho_c(\alpha_c)$.

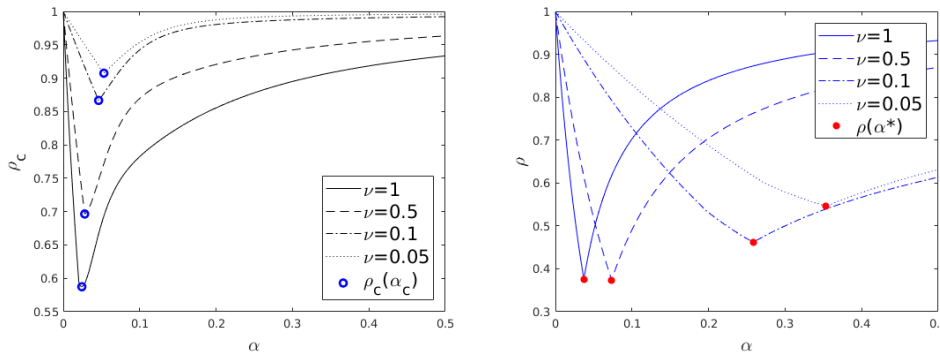


FIG. 5. Example 2: continuous (left) and discrete-time (right) convergence factors versus α , with α_c (blue circle) and α^* (red star), with $h_\Gamma = \Delta t = 1/24$; for $\nu = 1$ (solid line), $\nu = 0.5$ (dashed line), $\nu = 0.1$ (dash-dotted line), $\nu = 0.05$ (dotted line)

866

867 In Figure 6, we plot the evolution of the relative errors, of p , u_x and u_y , in
 868 the $L^\infty(0, T; L^2(\Omega))$ -norm, in logarithmic scale, after twenty OSWR iterations, as
 869 functions of the Robin parameter α . We also show the values of the errors obtained
 870 with optimized parameter $\alpha = \alpha_c$ (blue circle) and DT-optimized parameter $\alpha = \alpha^*$

871 (red star). The figures correspond to $\nu = 1$ (top left), $\nu = 0.5$ (top right), $\nu = 0.1$
 872 (bottom left), $\nu = 0.05$ (bottom right). We see that α^* is close to the numerical Robin
 873 value giving the smallest error after the same number of iterations, while α_c gives a
 larger error.

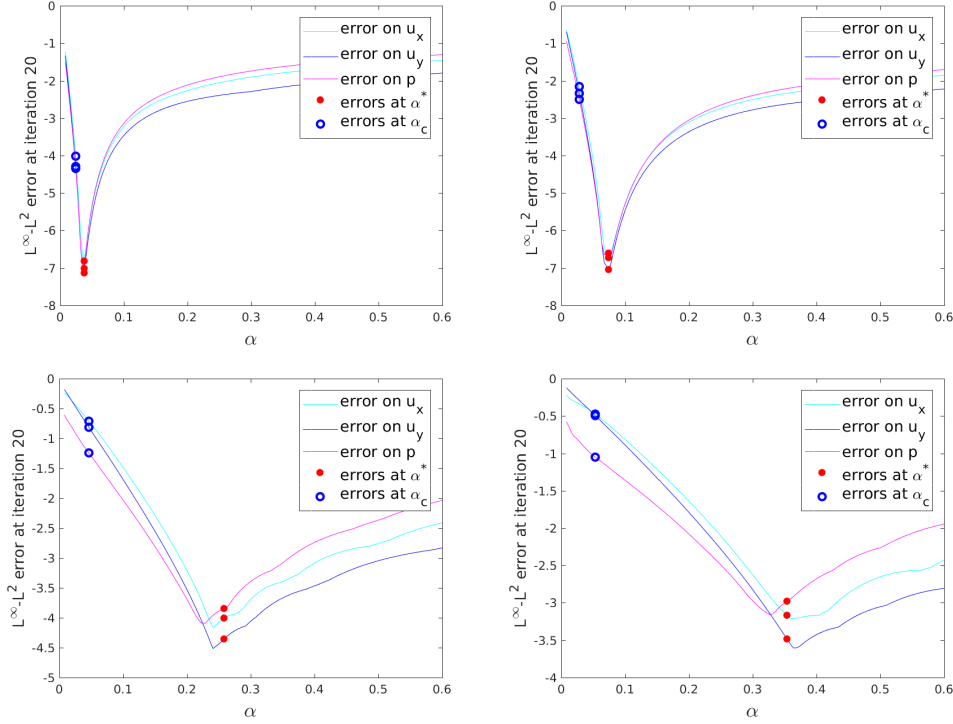


FIG. 6. *Example 2: Relative errors after 20 iterations (for u_x , u_y and p) versus α , with their values at α_c (blue circles) and at α^* (red stars), with $h_\Gamma = \Delta t = 1/24$; for $\nu = 1$ (top left), $\nu = 0.5$ (top right), $\nu = 0.1$ (bottom left), $\nu = 0.05$ (bottom right)*

874

875 **10.2.2. Case with ν fixed and different space-time meshes.** Let us take $\nu = 0.1$.
 876 In Figure 7, we plot the evolution of the continuous (left) and discrete-time (right)
 877 convergence factors, versus α , for different space-time meshes with $h_\Gamma = \Delta t = 1/12$
 878 (solid line), $h_\Gamma = \Delta t = 1/24$ (dashed line), and $h_\Gamma = \Delta t = 1/48$ (dash-dotted line).
 879 The theoretical optimized values α_c (blue circle) and α^* (red star) are also shown. We
 880 observe that both α_c and α^* decrease when the space-time mesh is refined. However,
 881 the values of α_c and α^* are again very different.

882 In Figure 8, we plot the relative errors, of p , u_x and u_y , in the $L^\infty(0, T; L^2(\Omega))$ -
 883 norm, after twenty OSWR iterations, versus Robin parameter α , for mesh 1 (top
 884 left), mesh 2 (top right), and mesh 3 (bottom). We also show the values of the errors
 885 obtained with $\alpha = \alpha_c$ (blue circle) and $\alpha = \alpha^*$ (red star). We observe that α^*
 886 is close to the numerical Robin value giving the smallest error after the same number of
 887 iterations, while α_c gives a larger error, for all space-time meshes considered.

888 **10.3. A more realistic test case.** In this example we take $\nu = \frac{1}{\mathcal{R}e}$ with $\mathcal{R}e = 200$,
 889 and $T = 5$. The mesh is given on Figure 9, with 22232 mesh elements. The domain is
 890 decomposed into two subdomains, with the interface at $y = -0.9$, see Figure 9, where

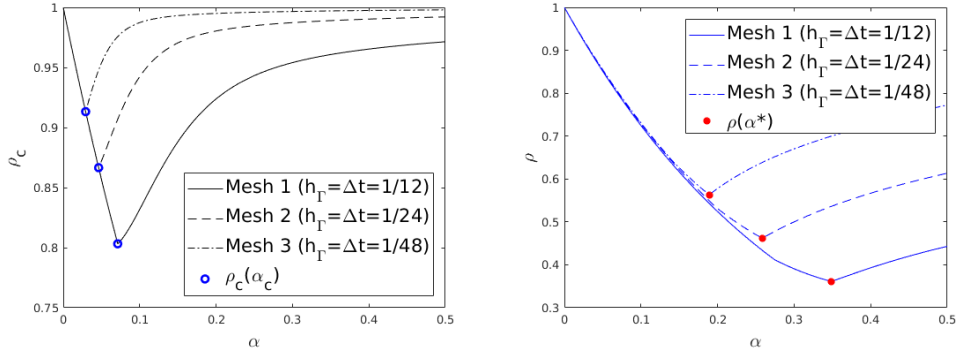


FIG. 7. Example 2: continuous (left) and discrete-time (right) convergence factors versus α , with α_c (blue circle) and α^* (red star), with $\nu = 0.1$; for $h_\Gamma = \Delta t = 1/12$ (solid line), $h_\Gamma = \Delta t = 1/24$ (dashed line), $h_\Gamma = \Delta t = 1/48$ (dash-dotted line)

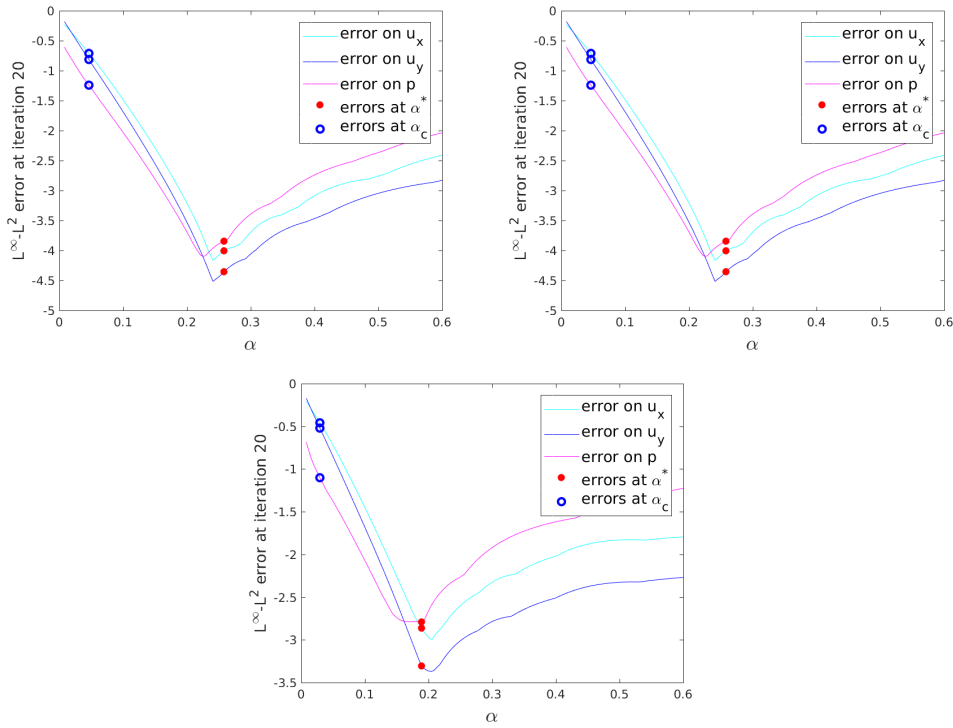


FIG. 8. Example 2: Relative errors after 20 iterations (for u_x , u_y and p) versus α , with their values at α_c (blue circles) and at α^* (red stars), with $\nu = 0.1$; for $h_\Gamma = \Delta t = 1/12$ (top left), $h_\Gamma = \Delta t = 1/24$ (top right), $h_\Gamma = \Delta t = 1/48$ (bottom)

891 domain 1 corresponds to the green and yellow parts, and domain 2 to the black part.
892 The time step is $\Delta t = 0.05$.

893 We set $\Omega_f = [-2.625, 1.625] \times [-0.9, -0.6]$, represented by the yellow part of the
894 mesh on Figure 9, and which corresponds to the location where the source term \mathbf{f} in
895 the Stokes equations does not vanish. Two different values for this source term will

896 be used in the numerical tests that follow.

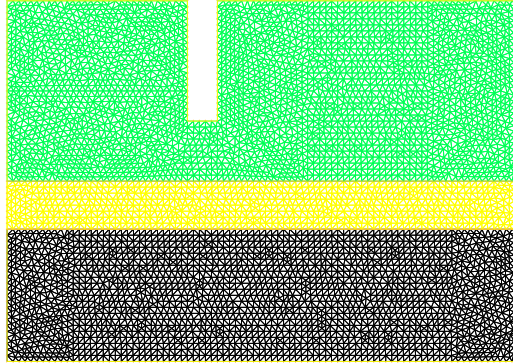


FIG. 9. *Example 3: mesh and domain decomposition*

897 In Figure 10, we plot the evolution of the continuous convergence factor ρ_c (left)
 898 and discrete-time convergence factor ρ (right), as functions of the Robin parameter α .
 899 The theoretical optimized values α_c (blue circle) and α^* (red star) are also shown,
 900 and their numerical values are $\alpha_c \approx 3.2283 \times 10^{-2}$ and $\alpha^* \approx 6.6063 \times 10^{-1}$, and differ
 901 from about a factor 20.

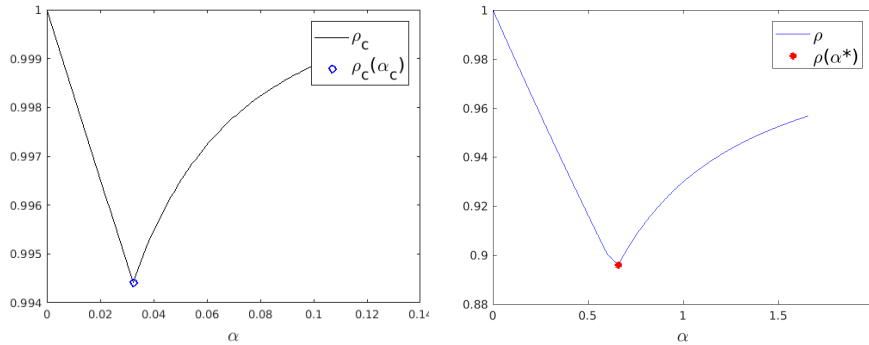


FIG. 10. *Example 3: continuous (left) and discrete-time (right) convergence factors versus α , with corresponding theoretical optimized values α_c (blue circle) and α^* (red star)*

902 In this example we consider two different source terms in $\Omega_f \times (0, T)$: a constant
 903 one: $\mathbf{f} = -2$, and then a variable in time one: $\mathbf{f} = -2(\sin(\pi t) + \cos(4\pi t))$.

904 In Figures 11 and 12, we plot the pressure p and the velocity field (u_x, u_y) re-
 905 spective, at times $t = 1$ and $t = T = 5$ (with a fixed color bar for p), for the case \mathbf{f}
 906 constant. We observe that the stationary state is not reached yet.

907 In Figure 13, we show the evolution of the relative errors, between the OSWR and
 908 monodomain solutions, of u_x , u_y , and p , in the $L^\infty(0, T; L^2(\Omega))$ -norm, as functions
 909 of OSWR iterations, for $\alpha = \alpha_c$ (cyan, green and blue curves) and $\alpha = \alpha^*$ (magenta,
 910 red, and black curves), with zero initial Robin data, with \mathbf{f} constant (left), and \mathbf{f}
 911 variable (right). For $\alpha = \alpha^*$, the curves of u_x and p are quite close, with a faster
 912 convergence for u_y . For $\alpha = \alpha_c$, the curves of u_x and u_y have almost the same speed of
 913 convergence, with a slower (resp. faster) convergence for p for the first iterations, for \mathbf{f}
 914 constant (resp. variable). Moreover, the convergence is much slower with $\alpha = \alpha_c$ than

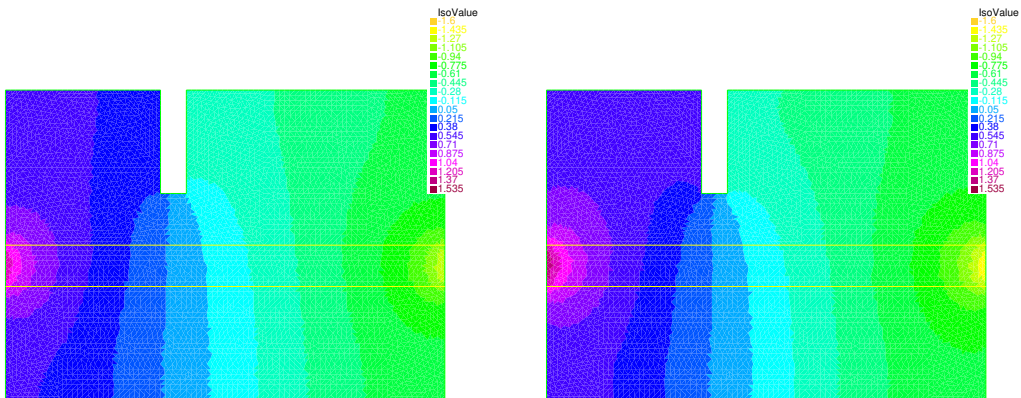


FIG. 11. *Example 3 (f constant): Pressure at $t = 1$ (left) and at final time $t = 5$ (right)*

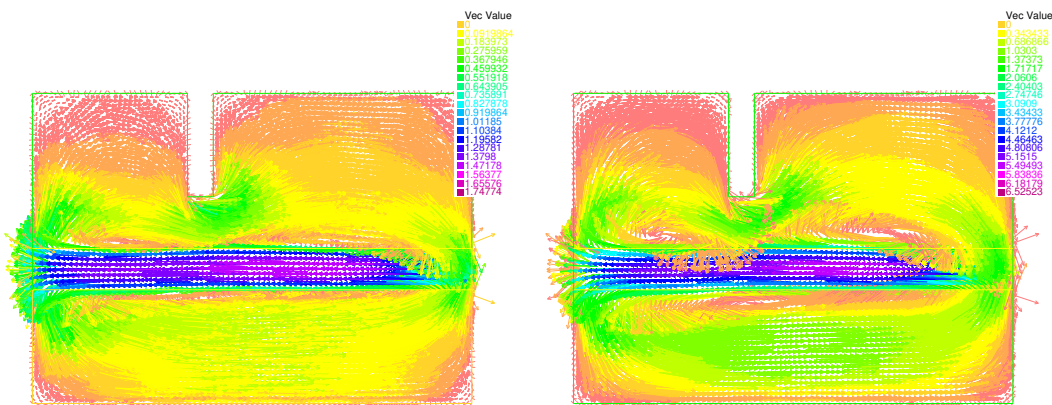


FIG. 12. *Example 3 (f constant): Velocity field at $t = 1$ (left) and at final time $t = 5$ (right)*

915 with $\alpha = \alpha^*$. This illustrates the importance of the effect of the numerical scheme
 916 used in the time direction.

917

REFERENCES

- 918 [1] S. ALI HASSAN, C. JAPHET, AND M. VOHRALÍK, *A posteriori stopping criteria for space-time*
 919 *domain decomposition for the heat equation in mixed formulations*, ETNA, Electron. Trans.
 920 Numer. Anal., 49 (2018), pp. 151–181.
 921 [2] A. ARNOULT, C. JAPHET, AND P. OMNES, *Discrete-time analysis of Schwarz waveform re-*
 922 *laxation convergence*. working paper or preprint, available at [https://hal-univ-paris13.](https://hal-univ-paris13.archives-ouvertes.fr/hal-03746438/)
 923 [archives-ouvertes.fr/hal-03746438/](https://hal-univ-paris13.archives-ouvertes.fr/hal-03746438/), Aug. 2022.
 924 [3] E. AUDUSSE, P. DREYFUSS, AND B. MERLET, *Optimized Schwarz waveform relaxation for the*
 925 *primitive equations of the ocean*, SIAM J. Sci. Comput., 32 (2010), pp. 2908–2936.
 926 [4] D. BENNEQUIN, M. J. GANDER, AND L. HALPERN, *A homographic best approximation prob-*
 927 *lem with application to optimized Schwarz waveform relaxation*, Math. Comp., 78 (2009),

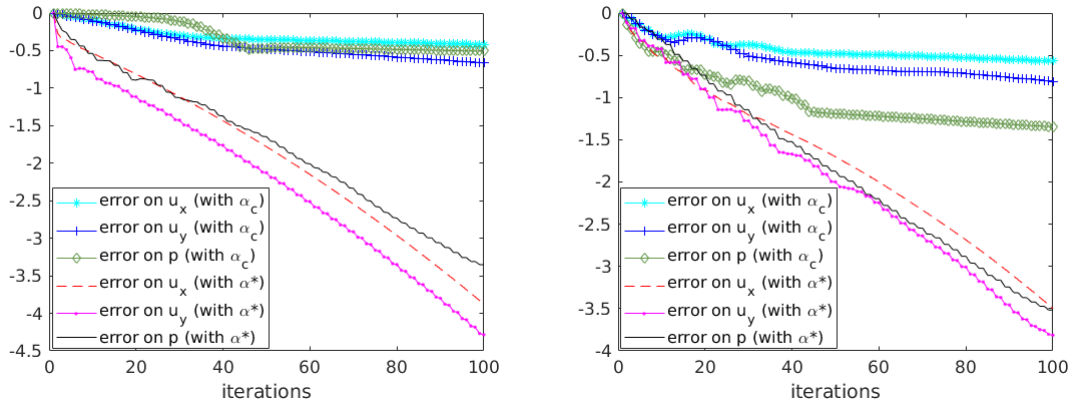


FIG. 13. *Example 3 : Relative errors of p , u_x , u_y , versus iterations, with optimized Robin parameters α_c (cyan, green and blue curves) and α^* (magenta, red, and black curves), with \mathbf{f} constant (left), and \mathbf{f} variable (right).*

- 928 pp. 185–223.
- 929 [5] P.-M. BERTHE, C. JAPHET, AND P. OMNES, *Space-time domain decomposition with finite vol-*
930 *umes for porous media applications*, in Domain decomposition methods in science and
931 *engineering XXI. Proceedings of the 21st international conference*, Inria Rennes Center,
932 *France, June 25–29, 2012*, Cham: Springer, 2014, pp. 567–575.
- 933 [6] E. BLAYO, D. CHEREL, AND A. ROUSSEAU, *Towards optimized Schwarz methods for the Navier-*
934 *Stokes equations*, *Journal of Scientific Computing*, 66 (2016), pp. 275–295.
- 935 [7] F. BOYER AND P. FABRIE, *Mathematical tools for the study of the incompressible Navier-Stokes*
936 *equations and related models*, Applied Mathematical Sciences, Springer New York, Nov.
937 2012.
- 938 [8] H. BREZIS, *Analyse fonctionnelle. Théorie et applications*, Mathématiques appliquées pour la
939 *maîtrise*, Masson, 1987.
- 940 [9] D. Q. BUI, *New space-time domain decomposition algorithms combined with the Parareal al-*
941 *gorithm*, PhD thesis, Thèse de doctorat, Mathématiques appliquées, Université Sorbonne
942 *Paris Nord*, 2021.
- 943 [10] D. Q. BUI, C. JAPHET, Y. MADAY, AND P. OMNES, *Coupling parareal with optimized Schwarz*
944 *waveform relaxation for parabolic problems*, *SIAM Journal on Numerical Analysis*, 60
945 (2022), pp. 913–939.
- 946 [11] T. CHACÓN REBOLLO AND E. CHACÓN VERA, *A non-overlapping domain decomposition method*
947 *for the Stokes equations via a penalty term on the interface*, *C. R., Math., Acad. Sci. Paris*,
948 334 (2002), pp. 221–226.
- 949 [12] D. CHEREL, *Décomposition de domaine pour des systèmes issus des équations de Navier-Stokes*,
950 *PhD thesis*, Université Grenoble Alpes, 2012.
- 951 [13] O. CIOBANU, L. HALPERN, X. JUVIGNY, AND J. RYAN, *Overlapping domain decomposition*
952 *applied to the Navier-Stokes equations*, in Domain Decomposition Methods in Science and
953 *Engineering XXII*, T. Dickopf, M. J. Gander, L. Halpern, R. Krause, and L. F. Pavarino,
954 *eds.*, Cham, 2016, Springer International Publishing, pp. 461–470.
- 955 [14] O. A. CIOBANU, *Méthode de décomposition de domaine avec adaptation de maillage en espace-*
956 *temps pour les équations d’Euler et de Navier-Stokes*, PhD thesis, Université Paris 13,
957 2014.
- 958 [15] S. CLEMENT, F. LEMARIÉ, AND E. BLAYO, *Discrete analysis of Schwarz waveform relaxation*
959 *for a diffusion reaction problem with discontinuous coefficients*, *SMAI J. Comput. Math.*,
960 8 (2022), pp. 99–124.
- 961 [16] M. DISCACCIATI, A. QUARTERONI, AND A. VALLI, *Robin-Robin domain decomposition methods*
962 *for the Stokes-Darcy coupling*, *SIAM J. Numer. Anal.*, 45 (2007), pp. 1246–1268.
- 963 [17] A. ERN AND J.-L. GUERMOND, *Theory and practice of finite elements*, Springer, New York,
964 2004.
- 965 [18] M. J. GANDER AND L. HALPERN, *Optimized Schwarz waveform relaxation methods for advection*
966 *reaction diffusion problems*, *SIAM J. Numer. Anal.*, 45 (2007), pp. 666–697.

- 967 [19] M. J. GANDER, L. HALPERN, AND F. NATAF, *Optimal Schwarz waveform relaxation for the one*
 968 *dimensional wave equation*, SIAM J. Numerical Analysis, 41 (2003), pp. 1643–1681.
- 969 [20] M. J. GANDER AND A. M. STUART, *Space-time continuous analysis of waveform relaxation for*
 970 *the heat equation*, SIAM J. Sci. Comput., 19 (1998), pp. 2014–2031.
- 971 [21] P. GERVASIO, A. QUARTERONI, AND F. SALERI, *Spectral approximation of Navier-Stokes equa-*
 972 *tions*, in Fundamental directions in mathematical fluid mechanics, Basel: Birkhäuser, 2000,
 973 pp. 71–127.
- 974 [22] E. GILADI AND H. B. KELLER, *Space-time domain decomposition for parabolic problems*, Numer.
 975 Math., 93 (2002), pp. 279–313.
- 976 [23] T. GOUDON, S. KRELL, AND G. LISSONI, *Non-overlapping Schwarz algorithms for the incom-*
 977 *pressible Navier-Stokes equations with DDFV discretizations*, ESAIM, Math. Model. Numer.
 978 Anal., 55 (2021), pp. 1271–1321.
- 979 [24] L. HALPERN, C. JAPHET, AND J. SZEFTTEL, *Optimized Schwarz waveform relaxation and dis-*
 980 *continuous Galerkin time stepping for heterogeneous problems*, SIAM J. Numer. Anal., 50
 981 (2012), pp. 2588–2611.
- 982 [25] L. HALPERN AND J. SZEFTTEL, *Nonlinear nonoverlapping Schwarz waveform relaxation for semi-*
 983 *linear wave propagation*, Math. Comput., 78 (2009), pp. 865–889.
- 984 [26] R. D. HAYNES AND K. MOHAMMAD, *Fully discrete Schwarz waveform relaxation on two bounded*
 985 *overlapping subdomains*, in Domain Decomposition Methods in Science and Engineering
 986 XXV, R. Haynes, S. MacLachlan, X.-C. Cai, L. Halpern, H. H. Kim, A. Klawonn, and
 987 O. Widlund, eds., Cham, 2020, Springer International Publishing, pp. 159–166.
- 988 [27] F. HECHT, *New development in freefem++*, J. Numer. Math., 20 (2012), pp. 251–265.
- 989 [28] T.-T.-P. HOANG, C. JAPHET, M. KERN, AND J. E. ROBERTS, *Space-time domain decomposition*
 990 *for advection-diffusion problems in mixed formulations*, Math. Comput. Simul., 137 (2017),
 991 pp. 366–389.
- 992 [29] T.-T.-P. HOANG AND H. LEE, *A global-in-time domain decomposition method for the coupled*
 993 *nonlinear Stokes and Darcy flows*, J. Sci. Comput., 87 (2021), p. 22. Id/No 22.
- 994 [30] C. JAPHET AND F. NATAF, *The best interface conditions for domain decomposition methods:*
 995 *absorbing boundary conditions*, Absorbing boundaries and layers, domain decomposition
 996 methods, Nova Sci. Publ., Huntington, NY, (2001), p. 348–373.
- 997 [31] O. A. LADYZHENSKAYA, *The Mathematical Theory of Viscous Incompressible Flow*, Gordon
 998 and Breach, Sciences Publishers, 1963.
- 999 [32] F. LEMARIÉ, L. DEBREU, AND E. BLAYO, *Toward an optimized global-in-time Schwarz algorithm*
 1000 *for diffusion equations with discontinuous and spatially variable coefficients. Part 2: The*
 1001 *variable coefficients case*, Electron. Trans. Numer. Anal., 40 (2013), pp. 170–186.
- 1002 [33] G. LISSONI, *DDFV method : applications to fluid mechanics and domain decomposition*, PhD
 1003 thesis, COMUE Université Côte d’Azur, 2019.
- 1004 [34] G. LUBE, L. MÜLLER, AND H. MÜLLER, *A new non-overlapping domain decomposition method*
 1005 *for stabilized finite element methods applied to the non-stationary Navier-Stokes equations*,
 1006 Numer. Linear Algebra Appl., 7 (2000), pp. 449–472.
- 1007 [35] V. MARTIN, *An optimized Schwarz waveform relaxation method for the unsteady convection*
 1008 *diffusion equation in two dimensions*, Appl. Numer. Math., 52 (2005), pp. 401–428.
- 1009 [36] V. MARTIN, *Schwarz waveform relaxation algorithms for the linear viscous equatorial shallow*
 1010 *water equations*, SIAM J. Scientific Computing, 31 (2009), pp. 3595–3625.
- 1011 [37] THE MATHWORKS, INC., *MathWorks help center*, Natick, Massachusetts, United States. Avail-
 1012 able at <https://fr.mathworks.com/help/matlab/ref/fminsearch.html>.
- 1013 [38] D. MEDKOVÁ, *Weak solutions of the Robin problem for the Oseen system*, J. Elliptic Parabol.
 1014 Equ., 5 (2019), pp. 189–213.
- 1015 [39] S. MONNIAUX AND E. M. OUHABAZ, *The incompressible Navier-Stokes system with time-*
 1016 *dependent Robin-type boundary conditions*, J. Math. Fluid Mech., 17 (2015), pp. 707–722.
- 1017 [40] L. MÜLLER AND G. LUBE, *A nonoverlapping DDM for the nonstationary Navier-Stokes prob-*
 1018 *lem*, ZAMM, Z. Angew. Math. Mech., 81 (2001), pp. 725–726.
- 1019 [41] F.-C. OTTO AND G. LUBE, *Non-overlapping domain decomposition applied to incompressible*
 1020 *flow problems*, in Domain decomposition methods 10. The 10th international conference,
 1021 Boulder, CO, USA, August 10–14, 1997, Providence, RI: AMS, American Mathematical
 1022 Society, 1998, pp. 507–514.
- 1023 [42] F.-C. OTTO AND G. LUBE, *A nonoverlapping domain decomposition method for the Oseen*
 1024 *equations*, Math. Models Methods Appl. Sci., 8 (1998), pp. 1091–1117.
- 1025 [43] F. C. OTTO, G. LUBE, AND L. MÜLLER, *An iterative substructuring method for div-stable finite*
 1026 *element approximations of the Oseen problem*, Computing, 67 (2001), pp. 91–117.
- 1027 [44] L. F. PAVARINO AND O. B. WIDLUND, *Balancing Neumann-Neumann methods for incompress-*
 1028 *ible Stokes equations*, Commun. Pure Appl. Math., 55 (2002), pp. 302–335.

- 1029 [45] R. RUSSO AND A. TARTAGLIONE, *On the Robin problem for Stokes and Navier–Stokes systems*,
1030 Math. Models Methods Appl. Sci., 16 (2006), pp. 701–716.
- 1031 [46] J. C. STRIKWERDA AND C. D. SCARBICK, *A domain decomposition method for incompressible*
1032 *viscous flow*, SIAM J. Sci. Comput., 14 (1993), pp. 49–67.
- 1033 [47] A. TARTAGLIONE AND G. STARITA, *A note on the Robin problem for the Stokes system*, Rend.
1034 Accad. Sci. Fis. Mat., Napoli (4), 68 (2001), pp. 129–138.
- 1035 [48] S. THERY, C. PELLETIER, F. LEMARIÉ, AND E. BLAYO, *Analysis of schwarz waveform relax-*
1036 *ation for the coupled ekman boundary layer problem with continuously variable coefficients*,
1037 Numerical Algorithms, 89 (2022), pp. 1145–1181.
- 1038 [49] X. XU, C. O. CHOW, AND S. H. LUI, *On nonoverlapping domain decomposition methods for the*
1039 *incompressible Navier-Stokes equations*, ESAIM: Mathematical Modelling and Numerical
1040 Analysis - Modélisation Mathématique et Analyse Numérique, 39 (2005), pp. 1251–1269.